Autumn College on Plasma Physics:
Long-Lived Structures and Self Organization in Plasmas.

Alfvén-wave dynamics

T. Passot
Observatoire de la Côte d'Azur, Nice

International Centre for Theoretical Physics, Trieste, 13 Oct. - 7 Nov. 2003

The work presented was done in collaboration with: P.L. Sulem
S. Champeaux, A. Gazol, D. Laveder

Outline:

I. Introduction: the Hall MHD equations and the linear waves
II. Alfvén waves in Hall MHD: linear instabilities
III. Nonlinear dynamics of long-wavelength Alfvén waves.
IV. Envelope dynamics.
V. Self-focusing instability: filamentation.
VI. Retaining kinetic effects in a fluid description of long Alfvén waves
VII. A Landau-fluid model for dispersive MHD waves.
VIII. Conclusion

I. Introduction

In a magnetized plasma, when dealing with phenomena involving frequency smaller or comparable to the ion cyclotron frequency $\Omega_i = \frac{Z_i e B}{c m_i}$ and scales smaller or comparable to the ion-inertial length $d_i = \frac{c_A}{\Omega_i}$, the dynamics can be described in the MHD approximation with the addition of the Hall term (ion inertia) in a generalized Ohm's law: $\mathbf{E} = -\frac{1}{c}\mathbf{u} \times \mathbf{B} + \frac{m_i}{ec\rho}\mathbf{j} \times \mathbf{B}$

Remarks : $n_i \approx n_e = n$, $\rho \approx m_i n$, $\mathbf{u} \approx \mathbf{u}_i$

ions and electrons move in a similar way (they separate at the scale d_i).

one can also write $\mathbf{E} = -\frac{1}{c}\mathbf{u}_e \times \mathbf{B}$

the magnetic field is frozen in the electron plasma: no reconnection possible.

Hall-MHD equations (in a non-dimensional form)
The state law is that of a polytropic gas $p \propto \rho^\gamma$:

$$\partial_t \rho + \nabla \cdot (\rho \mathbf{u}) = 0$$

$$\rho(\partial_t \mathbf{u} + \mathbf{u} \cdot \nabla \mathbf{u}) = -\frac{\beta}{\gamma} \nabla \rho^\gamma + (\nabla \times \mathbf{b}) \times \mathbf{b}$$

$$\partial_t \mathbf{b} - \nabla \times (\mathbf{u} \times \mathbf{b}) = \underbrace{-\frac{1}{R_i} \nabla \times \left(\frac{1}{\rho} (\nabla \times \mathbf{b}) \times \mathbf{b} \right)}_{\text{Hall term}}$$

$$\nabla \cdot \mathbf{b} = 0$$

$\beta = \frac{c_s^2}{c_A^2}$ $\quad c_A \equiv \frac{\mathcal{B}_0}{\sqrt{4\pi\rho_0}} = 1$ $\quad R_i = \frac{L}{d_i}$ $\quad$ where $\quad d_i \equiv \frac{c}{\omega_{pi}} = \frac{c_A}{\Omega_i}$

This MHD formalism is valid for a collisional plasma. It can also be used in the collisionless case provided β is not too large (smaller than unity). Results of the fluid limit are usually valid in the limit $\frac{m_e}{m_i} \ll \beta \ll \frac{T_e}{T_i}$. The assumption of a scalar pressure is a further simplification that can be questionable but which allows much simpler algebra.

One dimensional reduction

In a slab geometry, for oblique propagation, the MHD equations take the form

$$\frac{\partial \rho}{\partial t} + \frac{\partial(\rho u_x)}{\partial x} = 0$$

$$\frac{\partial u_x}{\partial t} + u_x \frac{\partial u_x}{\partial x} = -\frac{1}{\rho}\frac{\partial}{\partial x}\left(\frac{\rho^\gamma}{\gamma M_s^2} + \frac{|b|^2}{2M_a^2}\right)$$

$$\frac{\partial u}{\partial t} + u_x \frac{\partial u}{\partial x} = \frac{b_x}{M_a^2 \rho}\frac{\partial b}{\partial x}$$

$$\frac{\partial b}{\partial t} + \frac{\partial}{\partial x}(u_x b) = b_x \frac{\partial u}{\partial x} + i\sigma \frac{R_i}{M_a}\frac{\partial}{\partial x}\left(\frac{b_x}{\rho}\frac{\partial}{\partial x} b\right),$$

where :
x is the direction of propagation,
θ is the angle between $\hat{x}$ and $\mathbf{B_0}$,

$\mathbf{V} = u_x \hat{x} + u_y \hat{y} + u_z \hat{z}$; $u = u_y - i\sigma u_z$,

$\mathbf{B} = b_x\hat{x} + b_y\hat{y} + b_z\hat{z}$; $b = b_y - i\sigma b_z$,

sonic Mach number : $M_s = U_0/c_s$,

Alfvénic Mach number $M_a = \frac{U_0}{c_a}$,

$b_x = \cos\theta$ is a constant and $b_z(t = 0) = \sin\theta$,

U_0 is a typical speed used to adimentionalize the plasma velocity,

$\beta = \frac{c_s^2}{c_A^2}$,

$\sigma = \pm 1$.

In the dispersionless case three basic modes coexist: Alfvén and fast and slow magnetosonic waves.

Linear MHD waves (no dispersion):

$\rho = \rho_0 + \delta\rho \qquad \mathbf{b} = \mathbf{B}_0 + \delta\mathbf{b} \qquad \mathbf{u} = 0 + \mathbf{u}$

$$\partial_t \delta\rho + \nabla \cdot (\rho_0 \mathbf{u}) = 0$$

$$\partial_t \delta\mathbf{b} = \nabla \times (\mathbf{u} \times \mathbf{B}_0)$$

$$\partial_t \mathbf{u} = -\frac{\beta}{\rho_0}\nabla\delta\rho - \frac{\mathbf{B}_0}{\rho_0} \times (\nabla \times \delta\mathbf{b})$$

$$\nabla \cdot \delta\mathbf{b} = 0$$

For perturbations $\propto e^{i(kx-\omega t)}$, two types of waves

Alfvén waves : perturbations $\perp$ plane $(\mathbf{k}, \mathbf{B}_0)$

$$u_z = -\frac{1}{\sqrt{\rho_0}}\delta b_z \quad ; \quad \frac{\omega}{k} = c_A \cos\theta \quad ; \quad c_A = \frac{B_0}{\sqrt{\rho_0}}$$

c_A : Alfvén velocity ; c_s : sound velocity

Magneto-sonic waves : perturbations in plane $(\mathbf{k}, \mathbf{B}_0)$

$$\omega^4 - k^2(c_A^2 + c_s^2)\omega^2 + k^4 v_a^2 c_s^2 \cos^2\theta = 0$$

largest solution : FAST WAVE ; smallest solution : SLOW WAVE

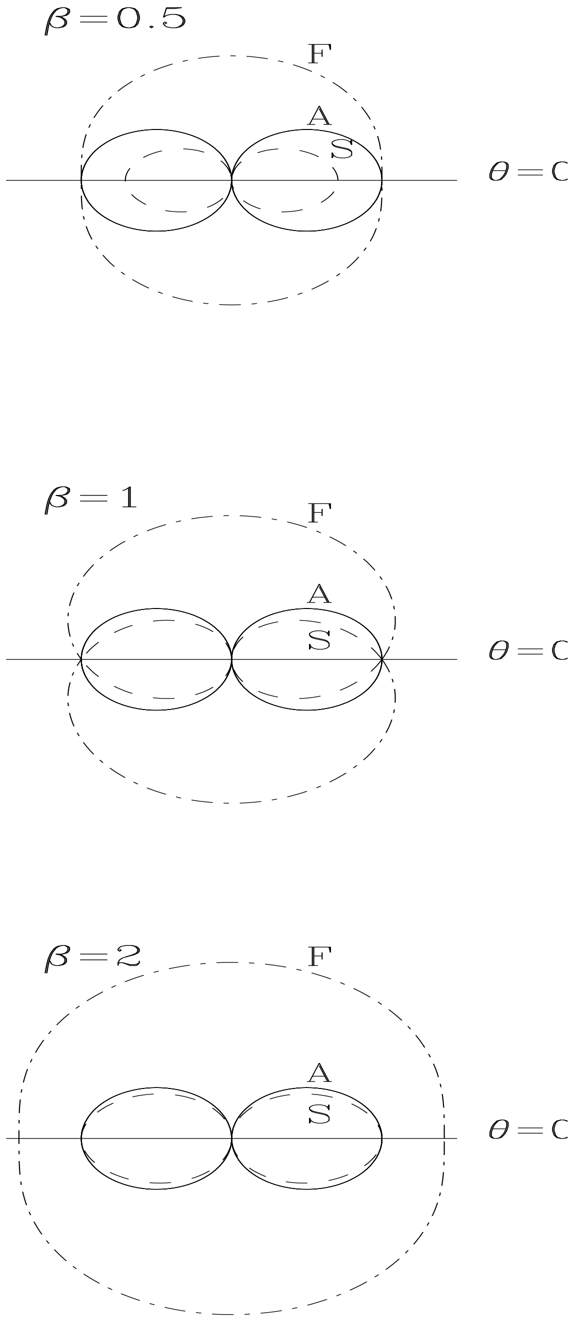

Figure 1: Polar diagram of the phase velocity ω/k

Physical interpretation of the magneto-sonic waves when $\beta \ll 1$:

- The fast wave is a transverse wave with perturbations along y-axis : *magnetic sound wave*.

- The slow wave corresponds to perturbations along the x-axis : *ion acoustic wave*.

When β is not small it is not possible to separate the magnetic sound from the ionic sound.

Propagation quasi-parallel to the ambient magnetic field:

The phase velocity of the Afvén wave and that of the fast ($\beta \ll 1$) or the slow ($\beta \gg 1$) magnetosonic wave identify : DEGENERACY : two modes are relevant in a **small dispersion** reductive perturbative expansion
$\Rightarrow$ equation for a **complex field**

II. Alfvén waves in Hall-MHD

Exact solutions: monochromatic, circularly polarized, parallel-propagating Alfvén waves

$$b_y - \sigma i b_z = -\frac{\omega}{k}(u_y - \sigma i u_z) = Be^{i(kx-\omega t)}$$

$$b_x = \rho = 1, \quad u_x = 0.$$

For forward propagation,

$$\omega = \frac{\sigma k^2}{2R_i} + k\sqrt{1 + \left(\frac{k}{2R_i}\right)^2}$$

Choosing $k > 0$, $\sigma = \pm 1$ for right-hand or left-hand polarization respectively.
Alfvén waves are then dispersive.

Dispersion relation $\omega(k)$ for parallel-propagating modes

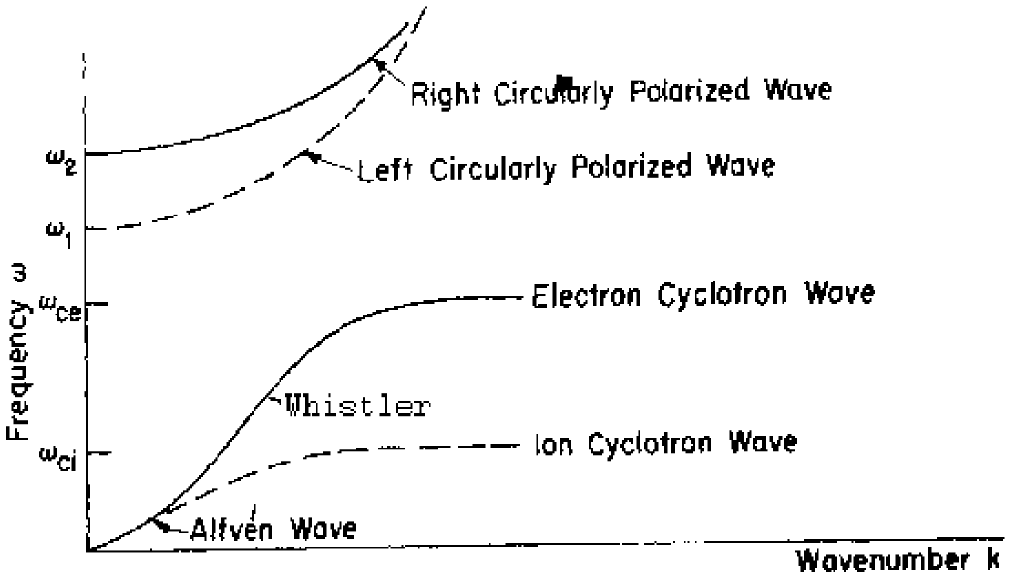

- LH Alfvén waves identify with ion-cyclotron waves for $\omega \lessapprox \Omega_i$.
- In the high-frequency (small-wavelength) limit, RH Alfvén waves identify with whistler modes:
  RH Alfvén Hall-MHD for $k^2 d_i^2 \gg 1 \longrightarrow \omega \approx k^2 c^2 \Omega_e / \omega_{pe}^2$
  $\approx$ whistler EMHD for $k^2 d_e^2 \ll 1$, where $d_e \equiv c/\omega_{pe}$
- In the non-dispersive limit $(k/R_i \rightarrow 0)$ the two modes become a shear-Alfvén branch (coinciding with a magnetosonic branch).
- Hall-MHD extends MHD to frequencies $\Omega \gtrsim \Omega_i$, with still $\Omega \ll \Omega_e$.

Direct observations of quasi-monochromatic dispersive almost circularly-polarized AW in the solar wind close to the Earth

(Spangler et al. JGR **93**, 845 (1988)). ISEE 1 and 2.

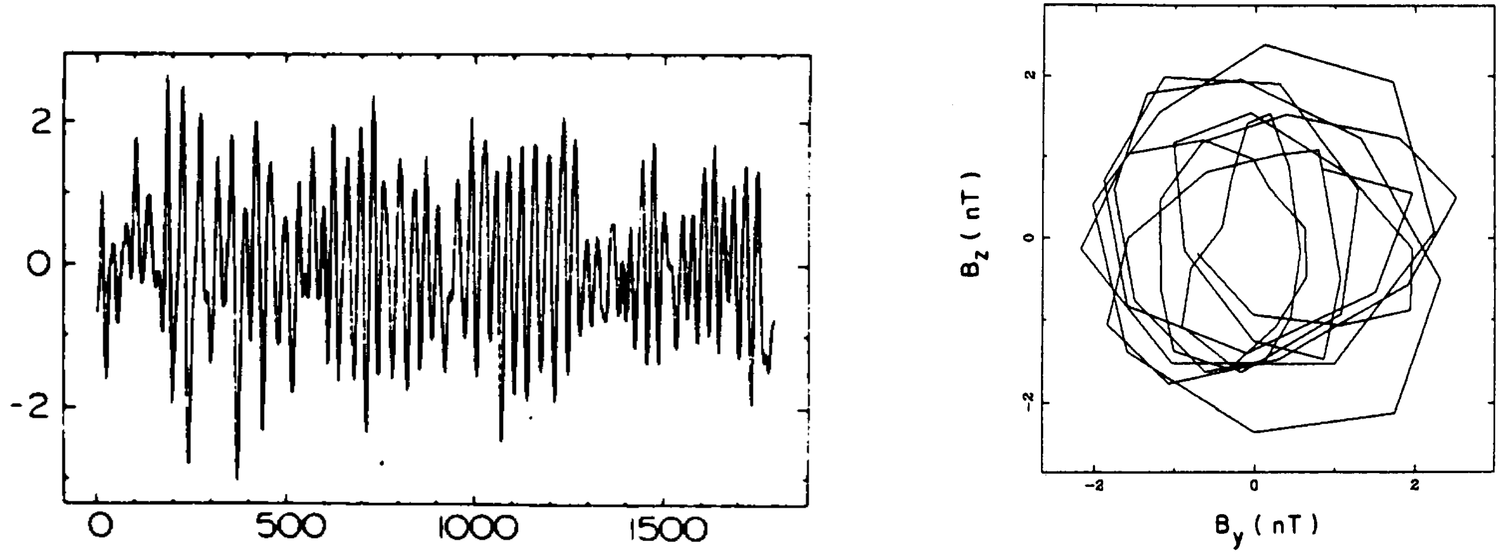

Figure 2: Time series of one magnetic field component (left) and plot of loci of the magnetic field components b_y and b_z on a time interval of 300 s. (right)

These MHD waves are excited by the reflected solar wind protons.

Instabilities $\Longrightarrow$ nonlinear effects :

$\Longrightarrow$ small scale formation $\Longrightarrow$ heating of the plasma

or

$\Longrightarrow$ formation of solitary structures

In order to distinguish between the different possibilities it is useful to study separately the finite wavelength perturbations and the long wavelength ones. In the latter case two different situations lead to asymptotic reductions: the long-wave limit (dispersion comparable to nonlinearity) and the situation of an amplitude modulation (finite dispersion, small amplitude limit).

General dispersion relation:

Linearization of the primitive MHD equations about an Alfvén wave of wavenumber k and amplitude b_0 (not restricted to be small), yields the dispersion relation

$$(\Omega^2 - \beta K^2)\mathcal{A}_+\mathcal{A}_- = \frac{b_0^2 K^2}{2}(\mathcal{A}_+\mathcal{C}_- + \mathcal{A}_-\mathcal{C}_+) \qquad (1)$$

where

$$\mathcal{A}_\pm = (\omega \pm \Omega)^2 - (k \pm K)^2 - \frac{\sigma}{R_i}(\omega \pm \Omega)(k \pm K)^2$$

$$\mathcal{C}_\pm = -k(k \pm K) - \frac{\sigma}{R_i}k(\omega \pm \Omega)(k \pm K)$$
$$+\frac{\Omega}{K}(\omega(k \pm K) + (\omega \pm \Omega)(k \pm K) - \frac{\sigma}{R_i}k^2(k \pm K)).$$

Following Wong and Goldstein (JGR **91**, 5617 (1986)), the instability is said modulational when it affects wave numbers $K < k$ (not necessarily asymptotically small), and decay when $K > k$.

Longitudinal dynamics of SMALL-AMPLITUDE waves

Pump wave : $e^{i(kx-\omega t)}$

Daughter wave : $e^{i(Kx-\Omega t)}$ Side-band waves : $e^{i[(k\pm K)x-(\omega\pm\Omega t)]}$

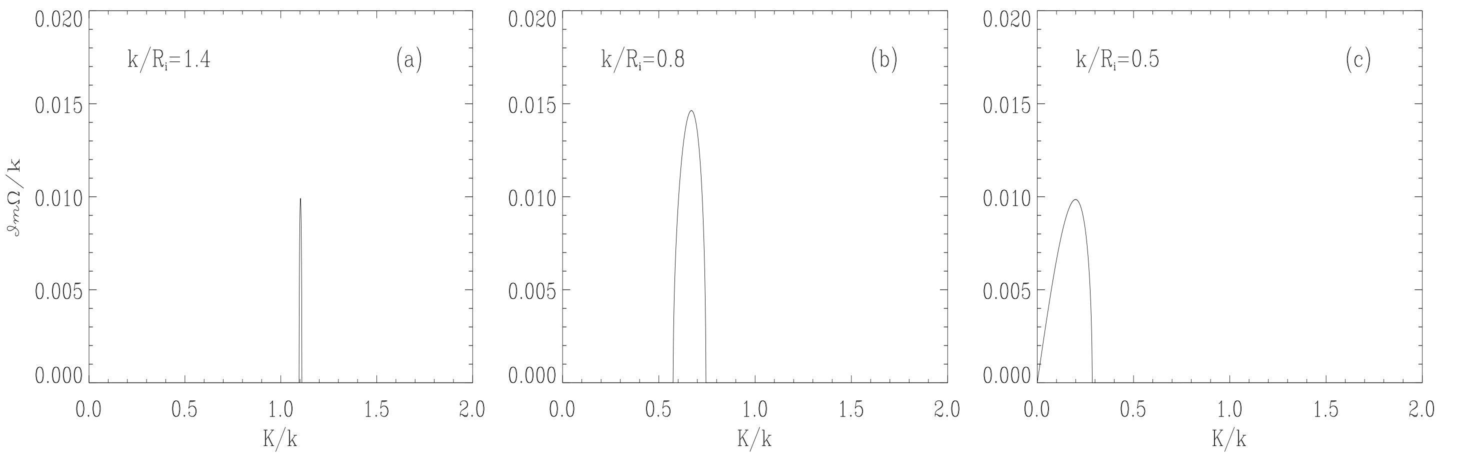

Figure 3: decay (a), modulational (b), long-wavelength modulational (c) instabilities (for RH polarized pump $\beta = 2.7$).

(a) Decay instability (forward Alfvén wave $\longrightarrow$ forward sound wave $+$ backward Alfvén wave): unstable wavenumbers $K > k$.

(b) Modulation instability: unstable wavenumbers $K < k$.

(c) Long-wavelength modulational instability extends to $K = 0$.

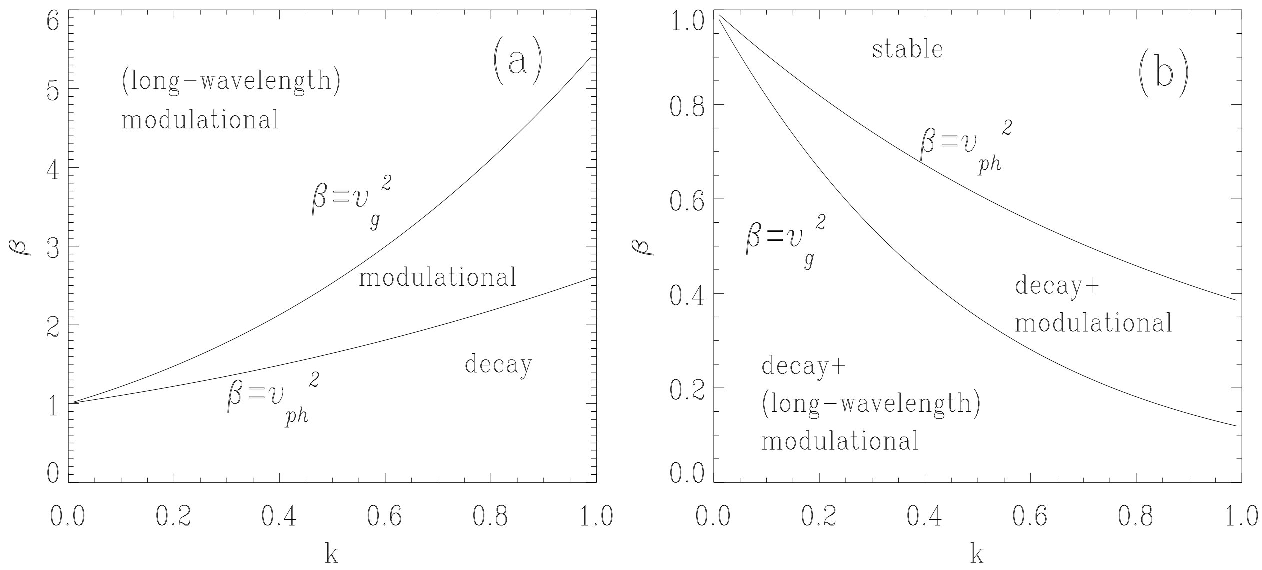

Figure 4: Longitudinal instability ranges for a small-amplitude right-hand (a) or left-hand (b) polarized Alfvén wave ($\beta = c_s^2$, $v_g = \frac{d\omega}{dk}$, $v_{ph} = \frac{\omega}{k}$).

Numerical resolution of the dispersion relation (1) for a carrier of small amplitude $b_0 \approx \epsilon B_0$ shows that for right-hand polarization the instability is modulational for $\beta > v_{ph}^2$ and of decay type for $\beta < v_{ph}^2$, where $v_{ph} = \omega/k$ is the phase velocity of the Alfvén wave. For left-hand polarization, the wave is stable for $\beta > v_{ph}^2$, while modulational and decay instabilities coexist for $\beta < v_{ph}^2$ (Fig. 4).

Note that, using Whitham formalism, one finds that waves are stabilized at large amplitude (Mjølhus, JPP **16**, 321 (1976)).

III. Nonlinear dynamics of long wavelength Alfvén waves

Long waves for which the dispersion is comparable to the nonlinearity are amenable to a reductive perturbative expansion. In the context of Alfvén waves propagating along an ambient magnetic field, due to the equality of the phase velocity of the Alfvén wave and of the speed of sound in the zero-dispersion limit, the latter asymptotics does not lead to the canonical Korteweg-de Vries equation but to the so-called "derivative nonlinear Schrödinger" (DNLS) equation for the two components of the magnetic field transverse to the propagation (Mjølhus, J. Plasma Physics **16**, 321 (1976), Mio et al. J. Phys. Soc. Japan **41**, 265 (1976), Kennel et al. Phys. Fluids **31**, 1949 (1988)). This approach concentrates on large-scale phenomena and neglects counterpropagating waves.

III.a Derivation of the multi-dimensional DNLS equation

We define the stretched variables $\xi = \epsilon(x-t)$, $\eta = \epsilon^{3/2}y$, $\zeta = \epsilon^{3/2}z$, and $\tau = \epsilon^2 t$ and expand

$$\rho = 1 + \epsilon\rho_1 + \epsilon^2\rho_2 + +\epsilon^3\rho_3 \cdots \tag{2}$$

$$u_x = \epsilon u_{x_1} + \epsilon^2 u_{x_2} + \epsilon^3 u_{x_3} + \cdots \tag{3}$$

$$b_x = 1 + \epsilon b_{x_1} + \epsilon^2 b_{x_2} + \epsilon^3 b_{x_3} + \cdots \tag{4}$$

$$u = \epsilon^{1/2}(u_1 + \epsilon u_2 + \epsilon^2 u_3 + \cdots) \tag{5}$$

$$b = \epsilon^{1/2}(b_1 + \epsilon b_2 + \epsilon^2 b_3 + \cdots). \tag{6}$$

At order $\epsilon^{3/2}$, we have

$$\partial_\xi u_1 + \partial_\xi b_1 = 0. \tag{7}$$

Equation (7) implies that the fluctuating parts (denoted by tildes) satisfy

$$\tilde{u}_1 = -\tilde{b}_1. \tag{8}$$

It is possible at this level to introduce mean (averaged over the ξ variable) transverse fields which can be shown to obey the reduced MHD equations. In the following, this coupling is ignored.

At order ϵ^2, we obtain

$$-\partial_\xi \tilde{\rho}_1 + \partial_\xi \tilde{u}_{x1} + \partial_\eta \tilde{u}_{y1} + \partial_\zeta \tilde{u}_{z1} = 0 \tag{9}$$

$$-\partial_\xi \tilde{b}_{x1} + \partial_\eta \tilde{u}_{y1} + \partial_\zeta \tilde{u}_{z1} = 0 \tag{10}$$

$$\partial_\xi(-\tilde{u}_{x1} + \beta\tilde{\rho}_1 + \frac{|\tilde{b}_1|^2}{2}) = 0 \tag{11}$$

$$\partial_\xi \tilde{b}_{x1} + \partial_\eta \tilde{b}_{y1} + \partial_\zeta \tilde{b}_{z1} = 0. \tag{12}$$

Using Eq. (8) we get

$$\partial_\xi \tilde{b}_{x1} + \partial_\eta \tilde{b}_{y1} + \partial_\zeta \tilde{b}_{z1} = 0 \tag{13}$$

Defining $\partial_\perp = \partial_\xi + i\partial_\eta$, Eqs. (9) then rewrite

$$\partial_\xi(-\tilde{\rho}_1 + \tilde{u}_{x1} + \tilde{b}_{x1}) = 0 \tag{14}$$

At order $\epsilon^{5/2}$, we obtain

$$\partial_\tau \tilde{b}_1 - \partial_\xi(\tilde{b}_2 + \tilde{u}_2) + \bar{b}_{x1}\partial_\xi \tilde{b}_1 + \partial_\xi \left(\tilde{b}_1(\tilde{u}_{x1} + \tilde{b}_{x1})\right) + \frac{i}{R_i}\partial_{\xi\xi}\tilde{b}_1 = 0. \tag{15}$$

Similarly, the equation for u_1 leads to

$$\partial_\tau \tilde{u}_1 - \partial_\xi(\tilde{u}_2 + \tilde{b}_2) + \partial_\xi \left(\tilde{b}_1(\tilde{\rho}_1 - \tilde{u}_{x1} - \tilde{b}_{x1})\right)$$
$$+(\bar{\rho}_1 - \bar{u}_{x1} - \bar{b}_{x1})\partial_\xi \tilde{b}_1 + \partial_\perp(\beta\tilde{\rho}_1 + \tilde{b}_{x1} + \frac{|\tilde{b}_1|^2}{2}) = 0 \tag{16}$$

Here the overbar means average over the longitudinal variable. The solvability condition for eqs. (15) and (16) leads to

$$\partial_\tau \tilde{b}_1 + \partial_\xi \left((-\frac{\tilde{\rho}_1}{2} + \tilde{u}_{x1} + \tilde{b}_{x1})\tilde{b}_1\right) + (-\frac{\bar{\rho}_1}{2} + \bar{u}_{x1} + \bar{b}_{x1})\partial_\xi \tilde{b}_1$$
$$-\frac{1}{2}\partial_\perp\left(\beta\tilde{\rho}_1 + \tilde{b}_{x1} + \frac{|\tilde{b}_1|^2}{2}\right) + \frac{i}{2R_i}\partial_{\xi\xi}\tilde{b}_1 = 0, \tag{17}$$

which generalizes the usual DNLS equation by the presence of coupling to longitudinal mean fields. While, to leading order, the fluctuating fields entering eq. (17) have been determined by the equations obtained at order ϵ^2, the computation of the mean fields requires to push the expansion to order ϵ^3. Defining $\delta = \rho - b_x$, we get

$$\partial_\tau \bar{\delta}_1 + \frac{1}{2}\left[\langle \partial_\perp^*(\tilde{b}_1(\tilde{u}_{x1} - \tilde{\delta}_1))\rangle + c.c.\right] = 0 \tag{18}$$

and

$$\partial_\tau \bar{u}_{x1} + \frac{1}{2}\left[-\langle\partial_\perp^*(\tilde{b}_1(\tilde{b}_{x1} + \tilde{u}_{x1}))\rangle + c.c.\right] = 0. \tag{19}$$

Eliminating $\tilde{\delta}_1$ and $\tilde{u}_{x1}$, by using eqs. (11) and (14), using the divergenceless conditions for $\tilde{b}$ in order to simplify eq. (17), and dropping the subscripts, one finally gets

$$\partial_\tau \tilde{b} + \partial_\xi\left(\frac{1}{2}\tilde{b}\tilde{P} + (\bar{u}_x + \frac{1}{2}\bar{b}_x - \frac{1}{2}\bar{\delta})\tilde{b}\right) - \frac{1}{2}\partial_\perp \tilde{P} + \frac{i}{2R_i}\partial_{\xi\xi}\tilde{b} = 0$$

$$\partial_\xi \tilde{b}_x + \frac{1}{2}\left(\partial_\perp^* \tilde{b} + c.c.\right) = 0 \tag{20}$$

$$\partial_\tau \bar{\delta} = 0 \tag{21}$$

$$\partial_\tau \bar{u}_x = \frac{1}{2}\left(\partial_\perp^* \langle\tilde{b}\tilde{P}\rangle + c.c.\right) \tag{22}$$

$$\Delta_\perp\left((1+\beta)\bar{b}_x + \beta\bar{\delta} + \frac{|\tilde{b}|^2}{2}\right) = 0. \tag{23}$$

where $\tilde{P} = \frac{1}{2(1-\beta)}(2\tilde{b}_x + |\tilde{b}|^2 - \langle|\tilde{b}|^2\rangle)$.
For localized waves (Mjølus & Wyller '86, '88):

$$\partial_\tau b + \frac{1}{4(1-\beta)}\partial_\xi((|b|^2 + 2b_x)b) - \frac{1}{4(1-\beta)}\partial_\perp(|b|^2 + 2b_x) + \frac{i}{2R_i}\partial_{\xi\xi} b = 0$$

$$\partial_\xi b_x + \frac{1}{2}(\partial_\perp^* b + \partial_\perp b^*) = 0$$

III.b Properties of the DNLS equation in 1D

In 1D the mean fields are identically zero and the equation reads

$$\partial_\tau b + \frac{i}{2R_i}\partial_{\xi\xi} b + \frac{1}{4(1-\beta)}\partial_\xi(|b|^2 b) = 0 \tag{24}$$

which is integrable by inverse scattering (Kaup and Newell, J. Math. Physics, **19**, 798 (1978)).

(i) Modulational stability of a circularly polarized wave

The DNLS equation also admits an exact solution in the form of circularly polarized Alfvén waves $b = b_0 e^{-i\sigma(k\xi - \omega\tau)}$.

Linearization of the DNLS equation (24) about the above solution leads to the dispersion relation

$$\Omega^2 - 2K\left(\frac{\sigma k}{R_i} + \frac{b_0^2}{2(1-\beta)}\right)\Omega + \left(\frac{k^2}{R_i^2} - \frac{K^2}{4R_i^2} + \frac{3\sigma k b_0^2}{4R_i(1-\beta)} + \frac{3b_0^4}{16(1-\beta)^2}\right) = 0 \tag{25}$$

Equation (25) predicts a modulational instability for right-hand (left-hand) polarized waves when $\beta > 1 + \frac{b_0^2 R_i}{4k}$ (respectively $\beta < 1 - \frac{b_0^2 R_i}{4k}$).

On the primitive MHD equations, in the case of right-hand polarization, only the decay instability is present for $\beta < 1$. For $1 < \beta < 1 + \frac{b_0^2 R_i}{4k}$ the wave is stable, while for $\beta > 1 + \frac{b_0^2 R_i}{4k}$ it is modulationally unstable. In the case of left-hand polarization, modulational and decay instabilities coexist for $\beta < 1 - \frac{b_0^2 R_i}{4k}$, only the decay instability is present for $1 - \frac{b_0^2 R_i}{4k} < \beta < 1$ and the wave is stable for $\beta > 1$. The corresponding instability growth rates are shown on Fig. 5 for various values of β, together with the predictions of the DNLS models.

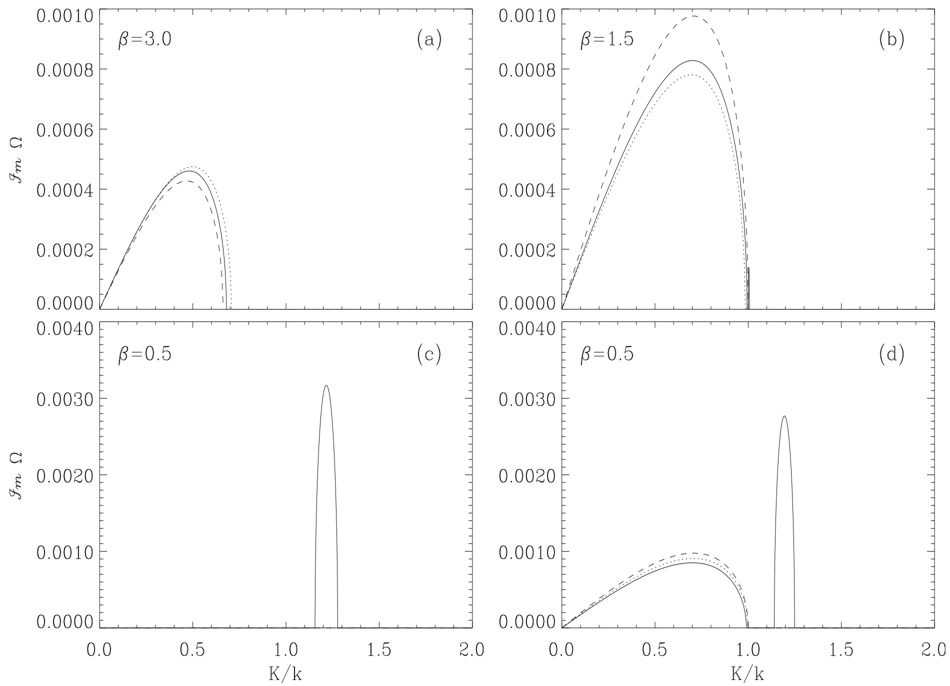

Figure 5: Instability growth rates (modulational and decay) for amplitude $\epsilon^{1/2} = 0.25$, $k = \epsilon = 0.0625$ at various β for right-hand polarization (panels (a)–(c)) and left-hand polarization (panel (d)), from the primitive MHD equations (solid line), the DNLS equation (24) (dashed line) and a non-adiabatic DNLS model (dotted line).

(ii) Two-parameter solitons

They form in the nonlinear stage of the modulation instability of the circularly polarized solutions. Rescale ξ so that $R_i = 1$. Mjølhus [1] found solitary wave packet solutions: $b = a \exp i\theta$ with real amplitude $a = a(x - vt)$ and phase θ. The local wavenumber $\kappa = \theta_x$ and frequency $\nu = -\theta_t$ obey, in a simple case:

$$a^2 = \frac{4(\nu_0 + \kappa_0)}{(\nu_0 + 2\kappa_0)^{1/2} \cosh\left[(x - vt - x_0)/\delta\right] + \kappa_0}$$

$$\kappa = \kappa_0 + (3/4)a^2 \qquad \delta^{-1} = 2(\kappa_0^2 + \nu_0)^{1/2}$$

$$\nu = \nu_0 + (3/4)a^2 \qquad v = -2\kappa_0$$

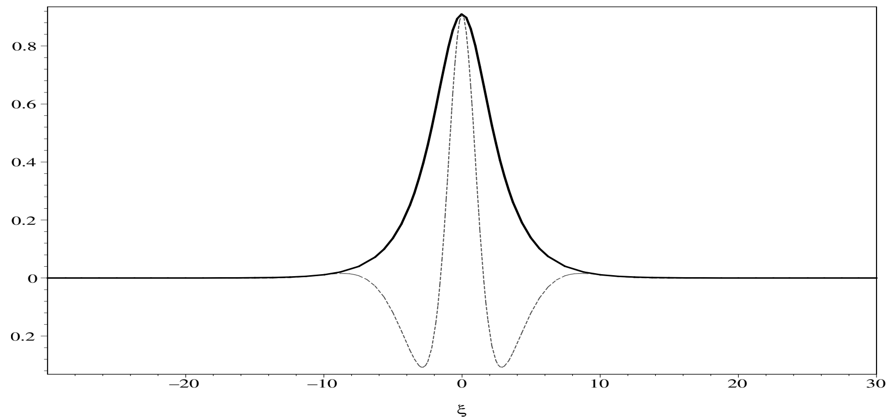

Figure 6: Envelope (solid) and real part (dotted) of the above soliton for $\kappa_0 = 0.5$, $\delta = 1$, $\nu_0 = 0$.

[1] Mjølhus and Hada in, *Nonlinear Waves in Space Plasmas*, eds. T. Hada and H. Matsumoto, Terrapub, Tokyo, 1997, p. 121

Perturbations

In the presence of a driver, the 1D DNLS equation can lead to chaos; RH soltions are more stable than LH ones. (Buti and Nocera, 1999).

Higher order nonlinearities also destroy the coherent properties of the DNLS solitons.

III.c The TRIPLE POINT $\beta = 1$

$\xi = \epsilon^{1/2}(x-t)$, $\eta = \epsilon y$, $\zeta = \epsilon z$, $\tau = \epsilon t$, write $\beta = 1 + \alpha\epsilon^{1/2}$ and expand

$$\rho = 1 + \epsilon^{1/2}\rho_1 + \epsilon\rho_2 + \epsilon^{3/2}\rho_3 \cdots$$

$$u_x = \epsilon^{1/2}u_{x_1} + \epsilon u_{x_2} + \epsilon^{3/2}u_{x_3} + \cdots$$

$$b_x = 1 + \epsilon^{1/2}b_{x_1} + \epsilon b_{x_2} + \epsilon^{3/2}b_{x_3} + \cdots$$

$$u = \epsilon^{1/2}(u_1 + \epsilon^{1/2}u_2 + \epsilon u_3 + \cdots)$$

$$b = \epsilon^{1/2}(b_1 + \epsilon^{1/2}b_2 + \epsilon^2 b_3 + \cdots).$$

Coupling to a Burgers type equation for the magnetosonic wave (Hada Geophys. Res. Lett. **20**, 2415 (1993)).

$\rho_1 = u_{x_1}$, $b_{x_1} = 0$. Dropping subscript index 1,

$$2\partial_T b + \partial_\xi(\rho b) - \partial_\perp \rho + \frac{i}{R_i}\partial_{\xi\xi} b = 0$$

$$2\partial_T \rho + \partial_\xi(\alpha\rho + \frac{\gamma+1}{2}\rho^2 + \frac{|b|^2}{2}) - \frac{1}{2}(\partial_\perp^* b + \partial_\perp b^*) = 0,$$

Webb, Brio & Zang, J. Plasma Phys. **54**, 201 (1995); J. Phys. A **29**, 5209.

Obliquely propagating Alfvén wave : non canonic

- The AW is compressive at dominant order if linearly polarized but can be almost incompressible in the case of arc or "banana" polarization.
- Nonlinearities vanish identically in the long-wave limit when the fields vary only along the direction of propagation
  $\longrightarrow$ dynamics reduces to linear dispersion (the same as for KdV) (Mio, Ogino & Takeda J. Phys. Soc. Japan **41**, 2114 (1976)).
- For nonlinear dynamics in one dimension, strong perturbations of the magnetic field component transverse to the propagation are required (Kakutani & Ono J. Phys. Soc. Japan **26**, 1305 (1969)): mKdV.
- In several dimensions, non canonic equations. Nonlinearities disappear in the limit of zero dispersion or for slowly varying perturbations in the transverse directions (Brodin J. Plasma Phys. **55**, 121 (1996); Gazol, Passot & Sulem J. Plasma Phys. **60**, 95 (1998).

IV. Envelope dynamics

Heuristic interpretation :

- **For LINEAR wave $Be^{i(kx-\omega t)}$, the dispersion relation reads**

$$(\omega - \Omega(k))\, B = 0 \quad \text{with} \quad B = \text{constant}$$

ω and k are associated to derivatives acting on $e^{i(kx-\omega t)}$.

- **With MODULATION and WEAK NONLINEARITIES:**

$B = B(X, Y, Z, T)$ **where** X, Y, Z, T **are slow variables.**

The dispersion relation becomes :

($\epsilon \sim$ `wave amplitude` $\sim$ `inverse scale of the modulation`)

$$\{\omega + i\epsilon\partial_T - \Omega(k - i\epsilon\partial_X, \epsilon\nabla_\perp, \epsilon^2|B|^2, \underbrace{\cdots}_{\text{mean fields}})\}B = 0$$

Dispersion enables computation of the harmonics in terms of the carrier

ϵ-expansion (amplitude and gradient expansion)

$\longrightarrow$ **Nonlinear Schrödinger equation :**

$$i\underbrace{(\partial_T + v_g\partial_X)B}_{\text{transport}} + \epsilon(\underbrace{\frac{v_g'}{2}\partial_{XX}B}_{\text{dispersion}} + \underbrace{p\Delta_\perp B}_{\text{diffraction}}) + \epsilon(q|B|^2 + \cdots)B = 0$$

(*eliminated by a change of frame*)

$$\frac{v_g'}{2v_g^2}\partial_{TT}B$$

Isotropic medium : $p = \frac{1}{2}\frac{\partial\Omega}{\partial k_y^2} = \frac{1}{2}\frac{\partial\Omega}{\partial k_z^2}|_{\mathbf{k}=k\mathbf{e}_x} = \frac{v_g}{2k}$, **with** $v_g = \frac{d\omega}{dk} =$ **group velocity**

Formal procedure

Use of a MULTIPLE-SCALE expansion

$$\partial_t \longrightarrow \partial_t + \epsilon\partial_T$$

$$\partial_x \longrightarrow \partial_x + \epsilon\partial_X$$

$$\partial_y \longrightarrow \epsilon\partial_Y$$

$$\partial_z \longrightarrow \epsilon \partial_Z$$

$$b = \epsilon b_1 + \epsilon^2 b_2 + \ldots$$

- $b_1 = B(X, Y, Z, T) e^{i(kx - \omega t)}$ solves the linear problem

$$\boxed{\mathcal{L}_0 b_1 = 0}$$

- Hierarchy of equations for higher order contributions:

$$\boxed{\mathcal{L}_0 b_i = \mathcal{F}_{i-1}} \qquad \mathrm{i} \geq 2$$

$\mathcal{F}_{i-1}$ given in terms of lower order harmonics.

Solvability conditions for $i = 2$ and $i = 3$

$\Longrightarrow$ **AMPLITUDE** equation.

IV.a The governing equations in 1D

The envelope equations governing the slow modulation of an Alfvén wave with a small (but finite) amplitude is obtained by a standard multiple-scale analysis (Champeaux, Passot & Sulem J. Plasma Physics **58**, 665 (1997)). Defining the slow variables $X = \epsilon x$ and $T = \epsilon t$ and expanding

$$u = \epsilon u_1 + \epsilon^2 u_2 + \epsilon^3 u_3 + \cdots, \; b = \epsilon b_1 + \epsilon^2 b_2 + \epsilon^3 b_3 + \cdots,$$
$$\rho = 1 + \epsilon^2 \rho_2 + \epsilon^3 \rho_3 + \cdots, \; u_x = \epsilon^2 u_2 + \epsilon^3 u_3 + \cdots,$$

To leading order

$$\partial_t u_1 - \partial_x b_1 = 0, \qquad \partial_t b_1 - \partial_x u_1 - i\frac{\sigma}{R_i}\partial_{xx} b_1 = 0. \tag{26}$$

The solution of Eq. (26) corresponds to a circularly polarized Alfvén wave $b_1 = -(\omega/k) v_1 = B_1 e^{i(kx-\omega t)}$ whose complex amplitude now depends on the slow variables.

Elimination of the secular oscillating terms in the equations at order ϵ^2 for the transverse fields leads to

$$\partial_T B_1 + v_g \partial_X B_1 = 0 \tag{27}$$

which expresses that B_1 is advected at the group velocity $v_g \equiv \omega' = \frac{2\omega^3}{k(k^2+\omega^2)}$. At order ϵ^3, the solvability condition of the equations for the transverse fields reads

$$i(\partial_T B_2 + v_g \partial_X B_2) + \mathcal{D} B_1 - k(\bar{u}_{x_2} - \frac{v_g}{2}\bar{\rho}_2) B_1 = 0 \tag{28}$$

where we introduced the dispersion operator

$$\mathcal{D} = \frac{\omega}{\omega^2 + k^2}\left(\frac{\omega^2}{k^2}\partial_{XX} + \frac{2k}{\omega}\partial_{XT} + \frac{k^2}{\omega^2}\partial_{TT}\right). \tag{29}$$

From Eq. (27), $\mathcal{D}B_1 = \frac{\omega''}{2}\partial_{XX}B_1$. Furthermore, overbars denote averaging over the fast variables.

Writing the equations obeyed by $\bar{u}_{x_2}$ and $\bar{\rho}_2$, and defining $B = B_1 + \epsilon B_2$ one gets, after dropping overbars and subscripts,

$$i(\partial_T + v_g\partial_X)B + \epsilon\frac{\omega''}{2}\partial_{XX}B - \epsilon k(u - \frac{v_g}{2}\rho)B = 0 \tag{30}$$

$$\partial_T\rho + \partial_X u = 0 \tag{31}$$

$$\partial_T u + \partial_X(\beta\rho + \frac{1}{2}|B|^2) = 0. \tag{32}$$

In the long-wavelength limit $k \longrightarrow 0$, this system reduces to that introduced by Ovenden et al. JGR **88**, 6095 (1983).

In the frame moving at the Alfvén-wave group velocity the above system rewrites, in terms of the coordinate $\xi = X - v_g T$ and of the slower time $\tau = \epsilon T = \epsilon^2 t$

$$i\partial_\tau B + \frac{\omega''}{2}\partial_{\xi\xi}B - k(u - \frac{v_g}{2}\rho)B = 0 \tag{33}$$

$$\epsilon\partial_\tau\rho + \partial_\xi(u - v_g\rho) = 0 \tag{34}$$

$$\epsilon\partial_\tau u + \partial_\xi(\beta\rho - v_g u + \frac{1}{2}|B|^2) = 0. \tag{35}$$

Neglecting the terms of order ϵ in Eqs. (34)–(35) make ρ and u slaved to the magnetic field amplitude, in the form $u = v_g \rho = \frac{v_g |B|^2}{2(v_g^2 - \beta)}$, (up to a constant in the periodic case). The long-wavelength modulation of the Alfvén wave envelope then obeys the nonlinear Schrödinger equation (NLS)

$$i\partial_\tau B + \frac{\omega''}{2}\partial_{\xi\xi} B + \frac{k v_g}{4(\beta - v_g^2)}|B|^2 B = 0. \tag{36}$$

This adiabatic approximation clearly breaks down near the resonance $\beta = v_g^2$, associated with the equality between the group velocity of the Alfvén wave and the speed of sound. Near this resonance, Eqs. (33)–(35) simplify through an additional rescaling. Keeping unchanged the magnitude of the transverse velocity and magnetic field and defining $\beta^{1/2} - v_g = \epsilon^{2/3}\lambda$, $\xi = \epsilon^{2/3}(x - v_g t)$, $\tau = \epsilon^{4/3} t$, and $u_x - \frac{v_g}{2}(\rho_M - 1) = \epsilon^{4/3}\phi$, one gets the Hamiltonian system derived by Benney (Stud. Appl. Math. **56**, 81 (1977)) in a general context

$$i\partial_\tau B + \frac{\omega''}{2}\partial_{\xi\xi} B - k\phi B = 0 \tag{37}$$

$$\partial_\tau \phi + \lambda \partial_\xi \phi = -\frac{1}{8}\partial_\xi |B|^2. \tag{38}$$

IV.b Linear stability analysis

The NLS equation (36) admits a solution with a constant amplitude B_0 and a phase that is uniform in space and linear in time. At the level of the primitive equations, it corresponds to a monochromatic Alfvén wave whose frequency is slightly shifted by the nonlinearity. Linearization about this solution leads to the dispersion relation

$$\Omega^2 = \frac{\omega''^2}{4} K^4 - \frac{k v_g \omega''}{4(\beta - v_g^2)} B_0^2 K^2, \tag{39}$$

which predicts a long-wavelength modulational instability for $\beta > v_g^2$ or $\beta < v_g^2$ according to the right-hand $(\omega'' > 0)$ or left-hand $(\omega'' < 0)$ carrier polarization.

NLS misses the modulational instability that occurs in the region of the plane $(\beta,\ k)$ between the two curves $\beta = v_g^2$ and $\beta = v_{ph}^2$. In this range of parameters, the unstable scales are too small to be accurately captured by the NLS asymptotics. In contrast, the dispersion relation for the envelope equations (30)–(32) predicts the persistence of the modulational instability for $\beta < v_g^2$ (right-hand polarization) or $\beta > v_g^2$ (left-hand polarization). The quantitative predictions for the range of unstable wave numbers and for the growth rates become nevertheless poorly accurate when β approaches v_{ph}^2, due to the loss of scale separation between the carrier and the unstable modes in this regime. The analysis can be refined by pushing the expansion to the next order in the modulational analysis.

IV.c Nonlinear dynamics

Simulations of the primitive MHD equations for $\beta = 4.0$, much in excess of the value $\beta \approx 3.2$ associated with the resonance $v_g = \beta^{1/2}$, show that in the nonlinear regime solitonic structures for the envelope of the transverse fields are formed (Fig. 7) and display a recurrent dynamics. Furthermore, as seen in Fig. 7, the density adiabatically follows the Alfvén wave intensity $\mathbf{b}^2 = b_y^2 + b_z^2$. As shown in Fig. 8, this dynamics is reproduced by the envelope equations (33)–(35), for which the adiabatic approximation is also verified. and which thus reduces to the NLS equation (from Champeaux et al. Nonlinear Proc. Geophys. **6**, 169 (1999))

Near the resonance $(\beta = 3.2)$ the dynamics is still of modulational type but the density no longer follow the variation of the magnetic field amplitude.

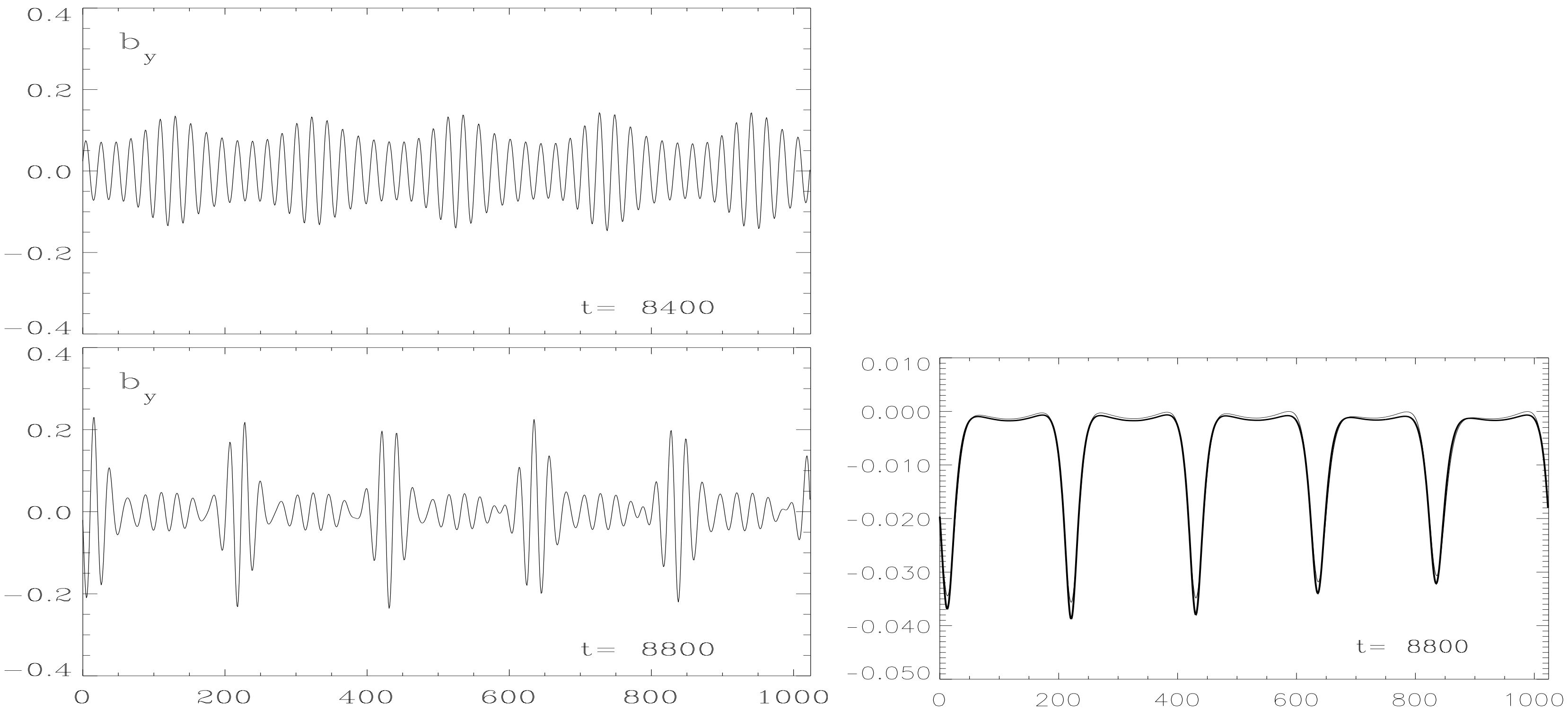

Figure 7: Snapshots of the magnetic field b_y (left) and of the density ρ (corrected by a constant) (right) from the primitive MHD equations with $\beta = 4.0$, for an initially weakly perturbed right-hand polarized wave of amplitude $\epsilon = 0.1$ and $k = 0.64$.

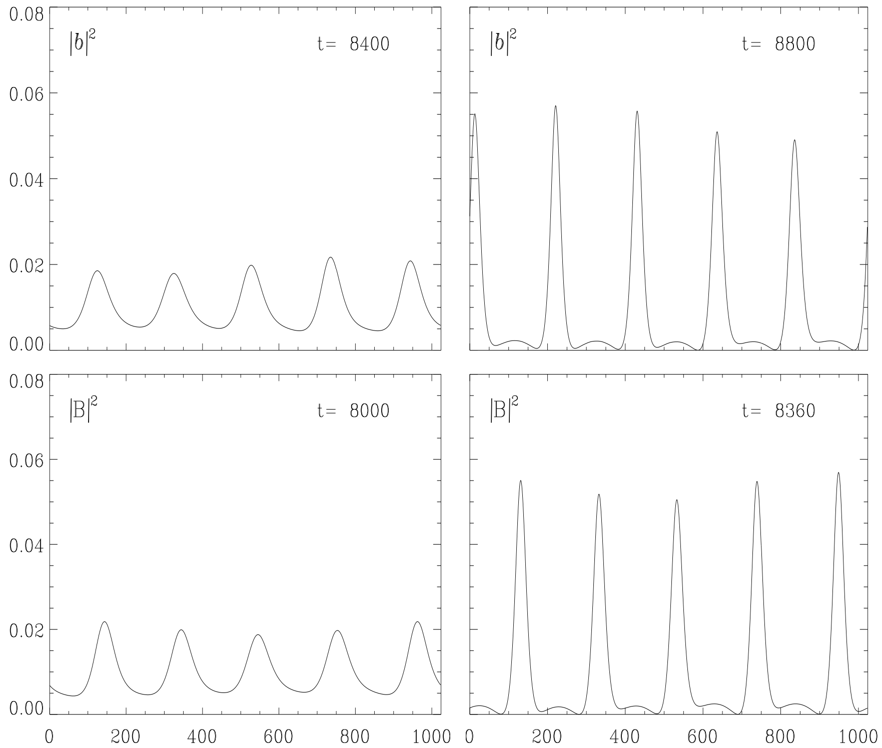

Figure 8: Comparison of the squared Alfvén wave intensity obtained from the primitive MHD equations in the laboratory frame (top), and the envelope equations (33)–(35) in the Alfvén wave frame (bottom), for $\beta = 4.0$, amplitude $\epsilon = 0.1$, $k = 0.64$ and right-hand polarization at comparable times (see text).

In the case $\beta = 2.45$, thus well beyond the resonance, the simulations of the MHD equations show that the dynamically relevant scales are not clearly separated from the carrier wavelength (Fig. 9). The envelope equations (33)–(35) can only provide a qualitative description of the dynamics, limited on a relatively short period of time. Even far from the resonance $v_g = \beta^{1/2}$, the adiabatic approximation does not hold and the MHD equations rapidly develop strong nonlinear phenomena, leading to density shocks (Fig. 9, where the small-scale oscillations are due to the Gibbs effect which develops in our non-dissipative code).

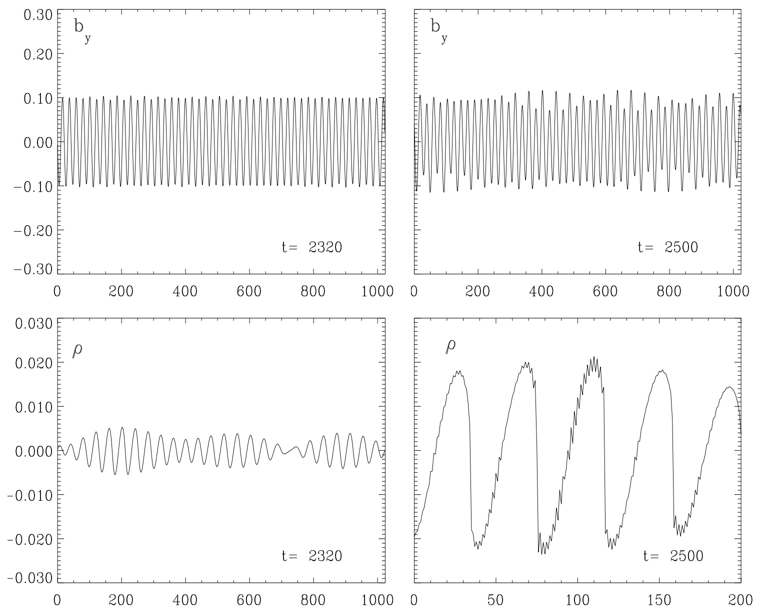

Figure 9: Snapshots of the magnetic field b_y (top) and of the density ρ (bottom) obtained from the primitive MHD equations, for $\beta = 2.45$, amplitude $\epsilon = 0.1$, $k = 0.64$ and right-hand polarization. Shocks are showed on a magnified scale.

As already mentioned, if the carrying wave is left-hand polarized, modulational and decay instabilities always coexist and the dynamics depends on the kind of instability that is prevalent. For a sufficiently small β the decay dominates the long-wavelength modulational instability (see Fig. 6), and strong nonlinearities rapidly develop, leading to small scales formation on the density field (Fig. 10, left). The modulational and decay growth rates become comparable when β slightly exceeds v_g^2. In this regime, the modulational instability affects scales that are not large enough to be accurately described by the envelope equations, and the corresponding evolution is seen in Fig. 10 (right). For larger β, the dynamics is governed by a modulational instability at scales comparable to that of the carrier, and density shocks rapidly form.

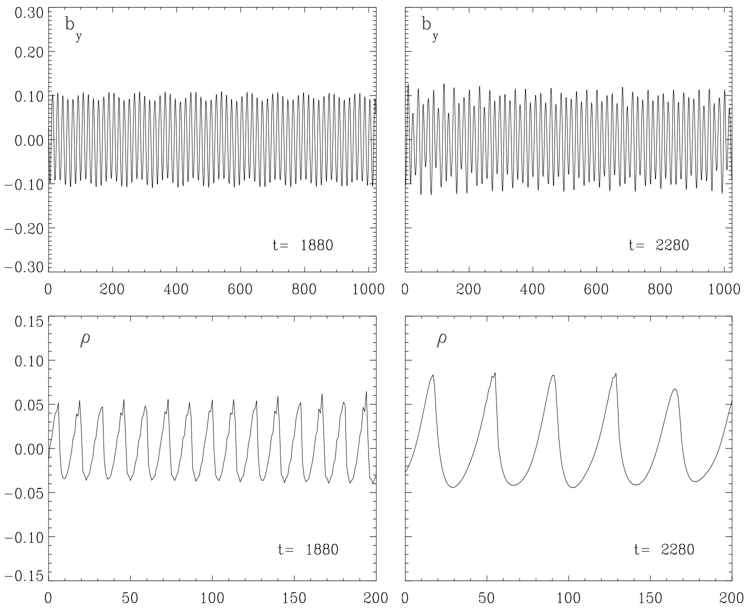

Figure 10: Snapshots of the magnetic field b_y (top) and, on a magnified scale, of the density ρ (bottom) obtained from the primitive MHD equations with $\beta = 0.21$ (left) and $\beta = 0.30$ (right), for amplitude $\epsilon = 0.1$, $k = 0.64$ and left-hand polarization.

IV.d Envelope dynamics in 3D

To select circularly polarized Alfvén waves, scale the transverse fields u_y, u_z, b_y, b_z like ϵ and the longitudinal fields $(\rho - 1, u_x, b_x)$ like ϵ^2. Define $\overline{\delta} = \overline{\rho} - \overline{b}_x$ where $\bar{\cdot}$ denotes averaging on the wave period.
Expend in powers of ϵ ; Define $X = \epsilon x$, $T = \epsilon t$

$$i(\partial_T B + v_g \partial_X B) + \epsilon \alpha \Delta_\perp B$$

$$+\epsilon \frac{\omega}{k^2+\omega^2}\left(\frac{\omega^2}{k^2}\partial_{XX}B + \frac{k^2}{\omega^2}\partial_{TT}B + \frac{2k}{\omega}\partial_{XT}B\right) \left\{ \begin{array}{l} \epsilon \frac{v_g'}{2}\partial_{XX}B \\ \epsilon \frac{v_g'}{2v_g^2}\partial_{TT}B \end{array} \right.$$

$$-\epsilon k v_g \left(\frac{1}{v_g}\bar{u}_x + \frac{k^2}{2\omega^2}\bar{b}_x - \frac{1}{2}\overline{\delta}\right)B = 0$$

$$\partial_T \overline{\delta} + \partial_X \bar{u}_x = 0$$

$$\partial_T \bar{u}_x + \beta \partial_X (\overline{\delta} + \bar{b}_x) + \partial_X \frac{|B|^2}{2} = \underbrace{-i\frac{\alpha}{v_g}\epsilon(B\Delta_\perp B^* - B^*\Delta_\perp B)}_{\frac{1}{v_g}(\partial_T + v_g \partial_X)|B|^2}$$

$$\partial_{TT}\bar{b}_x - \partial_{XX}\bar{b}_x - \Delta_\perp\left(\beta\overline{\delta} + (\beta+1)\bar{b}_x + \frac{k^2}{2\omega^2}|B|^2\right) = 0(\epsilon)$$

$$v_g = \omega' = \frac{2\omega^3}{k(k^2+\omega^2)} \quad ; \quad \alpha = \frac{k\omega}{k^2+\omega^2}\left(\frac{\omega^2}{2k^3} - \frac{1}{2}\frac{\beta k}{\beta k^2 - \omega^2}\right)$$

It is possible to take the limit $k \longrightarrow 0$ or $R_i \longrightarrow \infty$ in the coefficients. Equivalent to a modulation on DNLS equation.

Dispersion term :
$\frac{v_g}{2}\partial_{XX}B$ for an IVP in time (ABSOLUTE MODULATION)

$\frac{v_g'}{2v_g^2}\partial_{TT}B$ for IVP in space (CONVECTIVE MODULATION)

diffraction term : $\alpha\Delta_\perp B$ with $\alpha = \frac{1}{2}\frac{\partial^2\Omega}{\partial k_y^2} = \frac{1}{2}\frac{\partial^2\Omega}{\partial k_z^2}|_{\mathbf{k}=k\mathbf{e}_x}$

potential : $\mathcal{V} = -\frac{\delta\omega}{\delta\overline{\rho}}\overline{\rho} - \frac{\delta\omega}{\delta\overline{u}_x}\overline{u}_x - \frac{\delta\omega}{\delta\overline{b}_x}\overline{b}_x$

where $\omega = k(\epsilon\overline{u}_x + \frac{B_0+\epsilon\overline{b}_x}{\sqrt{1+\epsilon\overline{\rho}}})$ is the Doppler shifted frequency in the limit $k \longrightarrow 0$

ponderomotive forces : the term which appears subdominant rewrites $(\partial_T + v_g\partial_x)|B|^2$

and become **relevant for quasi-transverse perturbation** (transverse) *self-focusing* or *filamentation*.

The Hamiltonian character of the envelope equations prescribe the form of the ponderomotive force (Zakharov Rubenchik '72)

$$i\psi_t = -iv_g\psi_x - \frac{v_g'}{2}\psi_x x - \alpha\Delta_\perp\psi + (q|\psi|^2 + \mu\rho + \lambda\phi_x)\psi$$

$$\rho_t = -\rho_0\Delta\phi - \lambda|\psi|_x^2$$

$$\phi_t = -c^2\frac{\rho}{\rho_0} - \mu|\psi|^2$$

V. Self-focusing instability: filamentation

Whatever their polarization, monochromatic Alfvén waves are unstable relatively to transverse modulation

- $\boxed{\beta > \frac{\omega}{k} \approx 1 \text{ for small } k}$ the instability is ABSOLUTE

  i.e. develops in **time**.

  possibly affected by kinetic effects (P. and Sulem 2003)

- $\boxed{\beta < \frac{\omega}{k} \approx 1 \text{ for small } k}$ the instability is CONVECTIVE

  i.e. develops along the **direction of propagation**.

Nonlinear developments :

In the absolute regime: For a purely transverse modulation,

$$\bar{\rho} = \bar{b}_x, \quad \bar{u}_x = \frac{1}{v_g}|B|^2, \quad \bar{b}_x = -\frac{k^2}{2(\beta+1)\omega^2}|B|^2,$$

(up to additive numerical constants),
$\Longrightarrow$ 2d-NLS equation

$$i\partial_\tau B + \alpha \Delta_\perp B + r|B|^2 B = 0$$

$$\alpha = \frac{k\omega}{2(k^2+\omega^2)}\left(\frac{\omega^2}{k^3} - \frac{k\beta}{\beta k^2 - \omega^2}\right), \quad r = -kv_g\left(\frac{1}{v_g^2} - \frac{k^4}{4(\beta+1)\omega^4}\right), \quad v_g = \frac{d\omega}{dk}.$$

Usual two-dimensional NLS equation, modulational instability can lead to SELF-FOCUSING (or FILAMENTATION and WAVE-COLLAPSE : AMPLITUDE BLOW UP at localized foci.

Possible (transverse) WAVE COLLAPSE (blow-up of the NLS solution) $\Longrightarrow$ intense magnetic filaments parallel to the ambient magnetic field.

Mechanism leading to the filamentation process:

- the fluctuation of the Alfvén speed $v_A = \frac{B}{\sqrt{4\pi\rho}}$ during the filamentation process is given by

$$\bar{v}_A \approx \bar{u}_x + \frac{\bar{b}_x}{B_0} - \frac{1}{2}\frac{\bar{\rho}}{\rho_0} = \frac{4\beta + 3}{4(\beta+1)}|B|^2 > 0$$

- for β not too small ($\beta > 1$ in the long-wavelength limit), the wave amplitude grows where the transverse Laplacian of the wave phase $\Delta_\perp \phi > 0$: $\partial_t |B| = q^2(\beta)\Delta_\perp \phi$

v_A grows $\Rightarrow$ the wavefront gets curved to have $\Delta_\perp \phi > 0 \Rightarrow |B|$ grows $\Rightarrow v_A$ grows ...

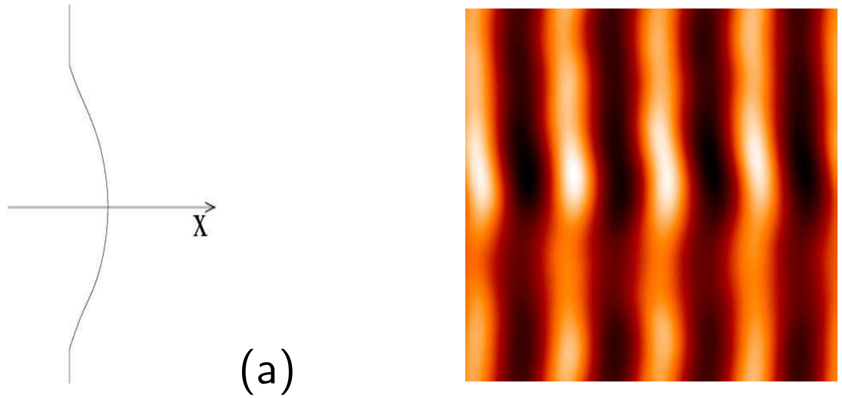

(a) (b)

This mechanism needs compressibility but not dispersion in principle. Dispersion is nevertheless essential to prevent longitudinal resonant coupling.

Such NLS solutions develop in such a way so as they invalidate the premises on which the multiple-scale expansion is based: The asymptotic description breaks down as the singularity is approached.

Near collapse, **damping processes**, not included in NLS,
come into play and dissipate the wave energy

⋆ How does the system leave the asymptotic regime?
⋆ Does the wave amplitude eventually saturate?
⋆ Influence of phenomena arising at other scales and eliminated by the asymptotics.
⋆ In particular, influence of the other instabilities that can compete with filamentation and possibly prevent it.

V.a Filamentation of a LH plane polarized Alfvén wave; Hall-MHD simulations

LH polarized pump, amplitude $B_0 = 0.1$, wavenumber $k/R_i = 1$, $\beta = 1.5$ (**no longitudinal instability.**)

Direct numerical simulations of 3D Hall MHD (Laveder, Passot & Sulem Phys. Plasmas **9**, 293 (2002)).

In order to concentrate on the action of the transverse instability
(and prevent significant excitation of the oblique instabilities),

⋆ only 4 pump wavelengths included in the computational box

⋆ dynamics initiated by density disturbances on small Fourier modes.

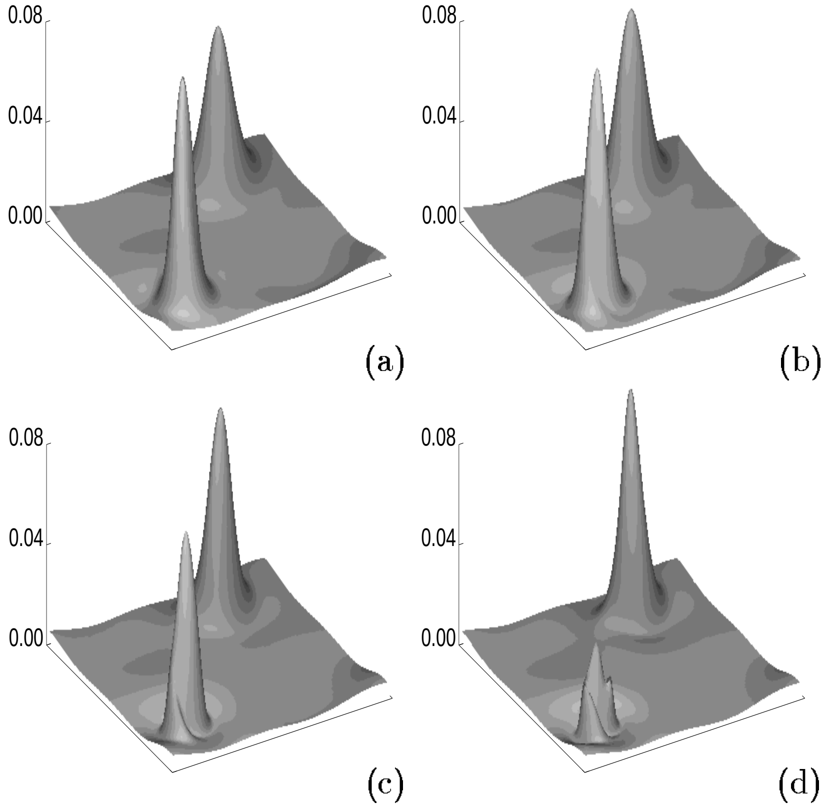

Figure 11: Amplitude of the transverse magnetic field intensity in a plane perpendicular to the propagation at times $t = 73.5$, 74, 74.8, 75.7.

Maximum amplification of the transverse magnetic-field intensity $\approx$ factor 10.

Nonlinear structures

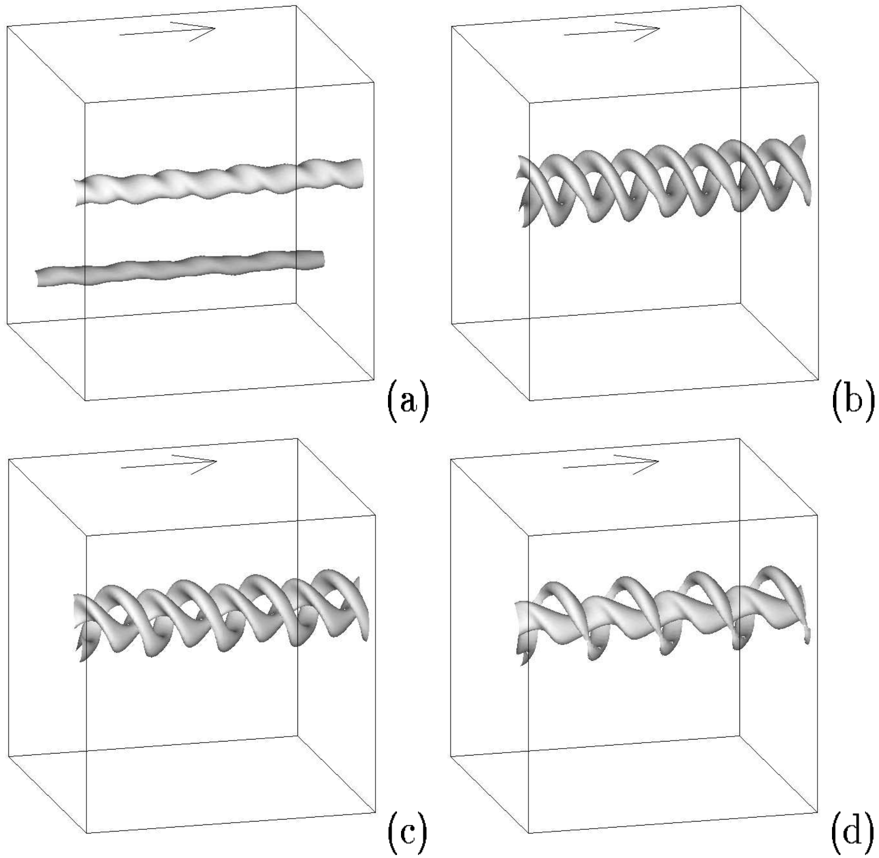

Figure 12: Isosurfaces (at $2/3$ of the extremal values) of the transverse magnetic field intensity $|b_\perp|^2 = b_y^2 + b_z^2$ (a), of the positive and negative density fluctuations $\rho - \rho_0$ (b), induced longitudinal magnetic field b_x (c) and longitudinal velocity u_x (d) at $t = 73.7$.

A regime of intense filamentation

LH polarized pump, amplitude $B_0 = 0.05$, wavenumber $\frac{k}{R_i} = 0.25$ (wave period $= 7.05$)

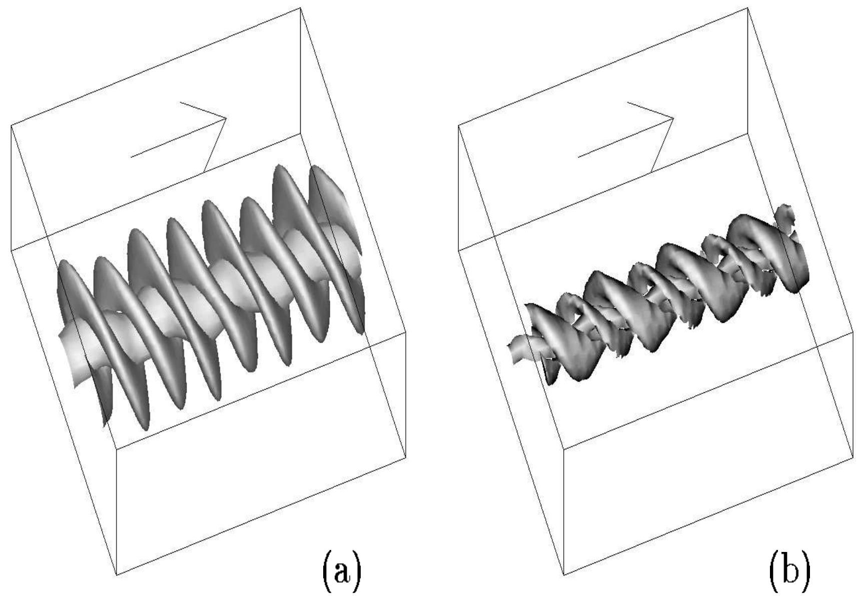

Figure 13: Isosurfaces of the transverse magnetic field intensity (inner tube) and of the positive and negative density fluctuations (helices) at $2/3$ of their extrema, at $t = 620$ (a) and 665 (b).

Local amplification of the wave intensity > 120 when 128^3-resolution becomes insufficient.

Density gradients are maximal inside the magnetic filament.

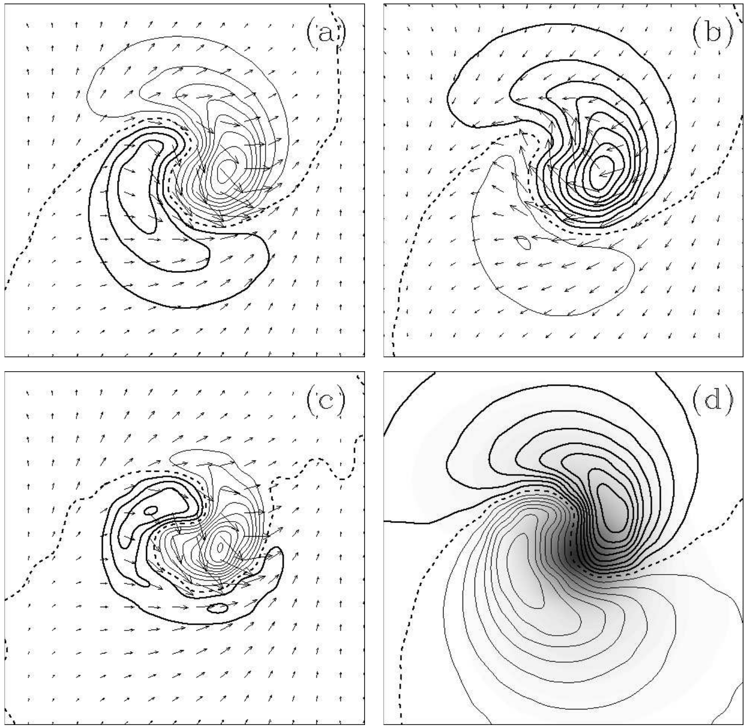

Figure 14: Transverse components (arrow) and longitudinal one (contours) of the magnetic field (a), velocity (b) and vorticity (c) in a plane perpendicular to the propagation, at $t = 665$. Panel (d) displays contours of positive and negative density fluctuations superimposed on the grey levels of the transverse magnetic field intensity. (Thick lines for positive contours, thin lines for negative ones and the dashed line for the zero-contour).

Electric field

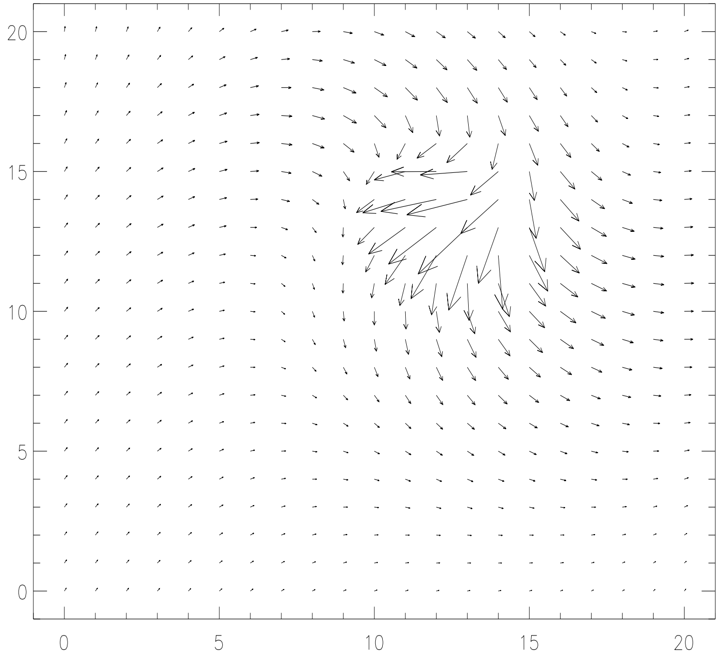

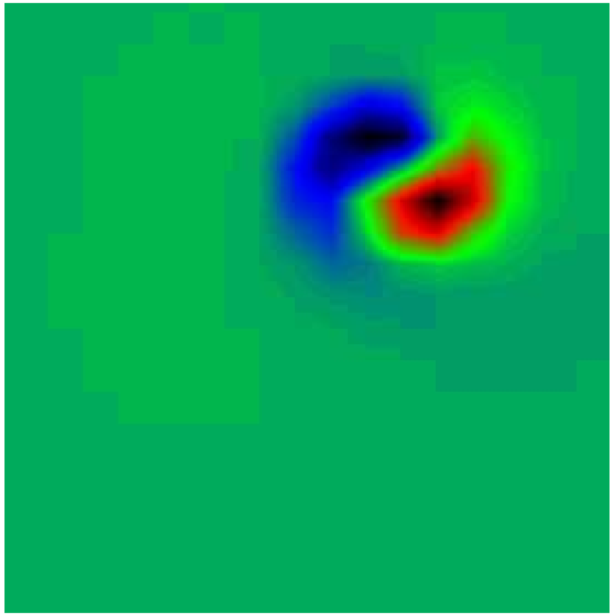

Comparison with amplitude-equation predictions

Mean fields:

$$\bar{\rho} = \bar{b}_x \qquad \bar{u}_x = \frac{1}{v_g}|B|^2 \qquad \bar{b}_x = -\frac{k^2}{2(\beta+1)\omega^2}|B|^2$$

Early collapse Late collapse

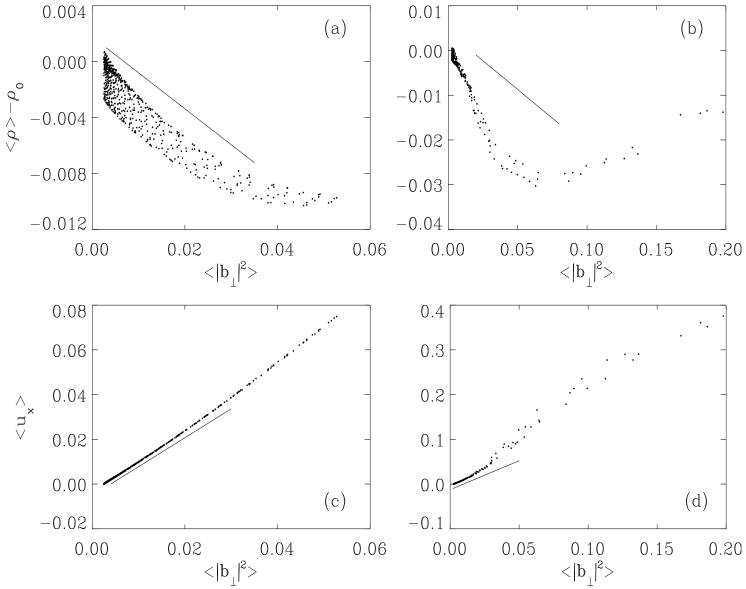

Figure 15: Plots of $\langle\rho\rangle - \rho_0$ (where ρ_0 is the unperturbed density) and $\langle u_x\rangle$ versus $\langle|b_\perp|^2\rangle$ at $t = 620$ (a, c) and $t = 665$ (b,d). The directions of the straight lines are given by the envelope equations.

What happens at later time?

For moderate amplitude initial AW saturation of the filamentation process takes place.
Below a certain amplitude, preliminary results (Grauer et al. using AMR simulations) indicate a possible finite-time singularity.

Oblique instabilities

Direct simulations:

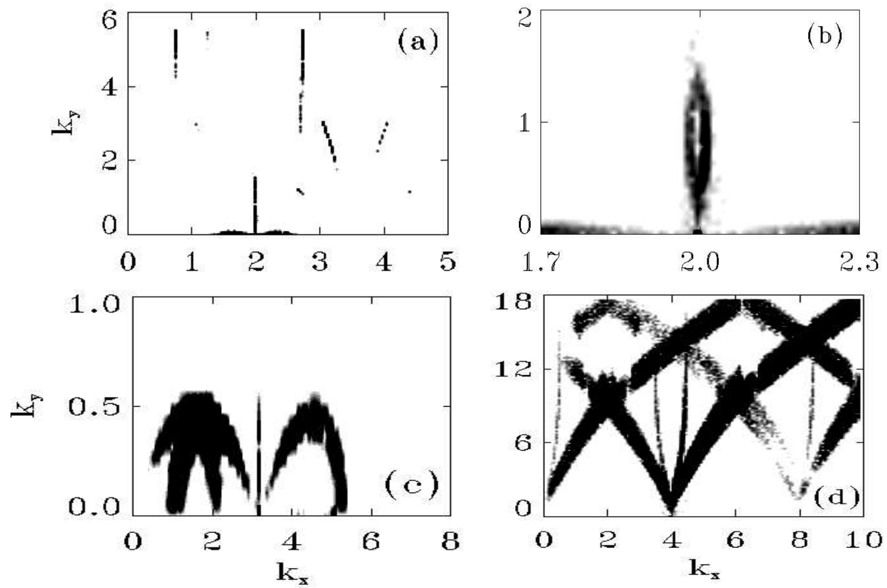

Figure 16: Spectral instability ranges of an Alfvén wave of amplitude 0.1 in various regimes: (a) RH polarization with $k = 2$ and $\beta = 2.7$; (b) details of (a) about the transverse unstable modes; (c) RH polarization with $k = 3.2$ and $\beta = 2.7$; (d) LH polarization with $k = 4$ and $\beta = 1.5$.

Envelope equations:

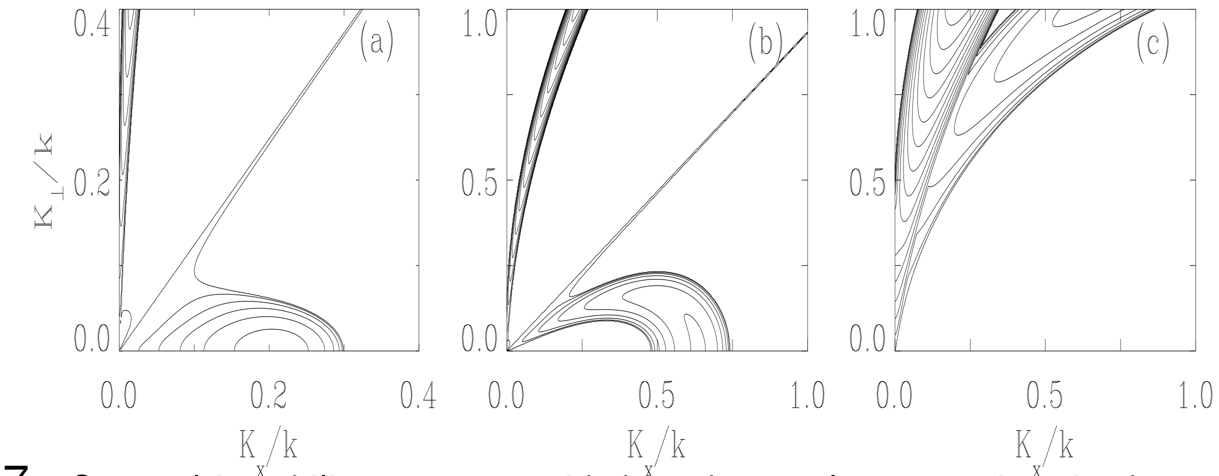

Figure 17: Spectral instability ranges provided by the envelope equations in the conditions of Figs. 8a, 8c and 8d (from left to right).

Spurious unstable oblique tails.

V.b Effect of quasi-transverse modes

Requires a large box in the longitudinal direction

Computational box including 16 pump wavelengths:

Parallel magnetic filaments first form but break at later times into a few segments oriented along oblique directions.
Filamentation proceeds after breaking.

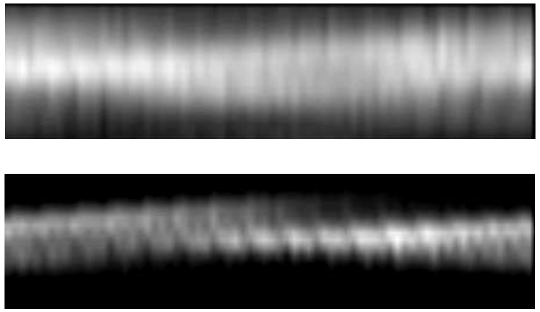

Figure 18: Magnetic filament before breaking ($t = 520$, upper panel) and after breaking ($t = 600$, lower panel).

Transverse magnetic field intensity locally amplified by a factor 100 before 128^3-resolution becomes insufficient.

Computational box including 32 pump wavelengths:

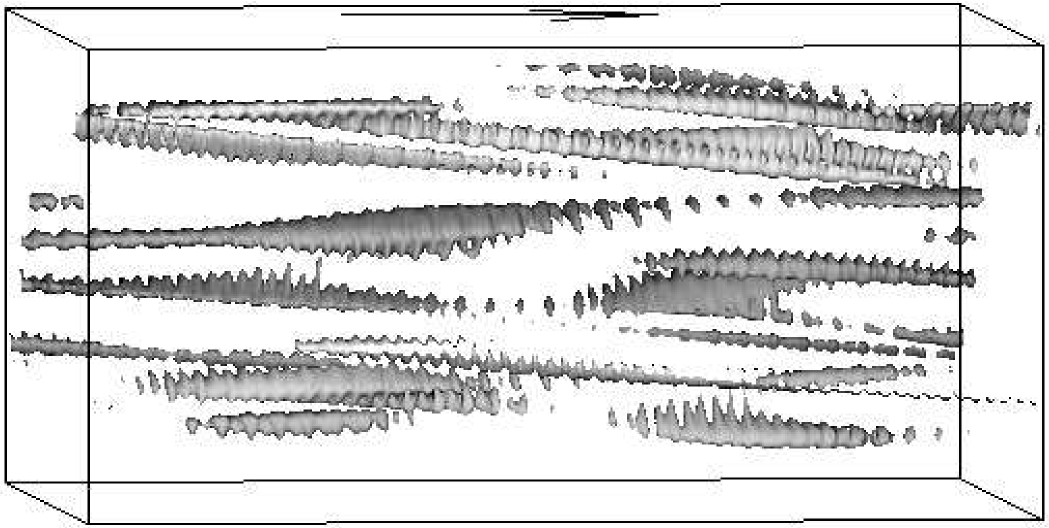

Figure 19: Isosurface of the transverse magnetic field intensity at $1/3$ of the maximum at $t = 480$.

Oblique filaments are formed

Transverse magnetic field intensity locally amplified by a factor 12 when the 512×128^2-resolution becomes insufficient.

V.c Three dimensional wave packet: non-monochromatic Alfvén beam

Is a non-monochromatic wave collapsing?

$\Longrightarrow$ only "sufficiently monochromatic" wave packets can develop filamentary structures.

Simulation of the 3D amplitude equations (128^3) (Laveder et al. Physica D **184**, 237 (2003)):

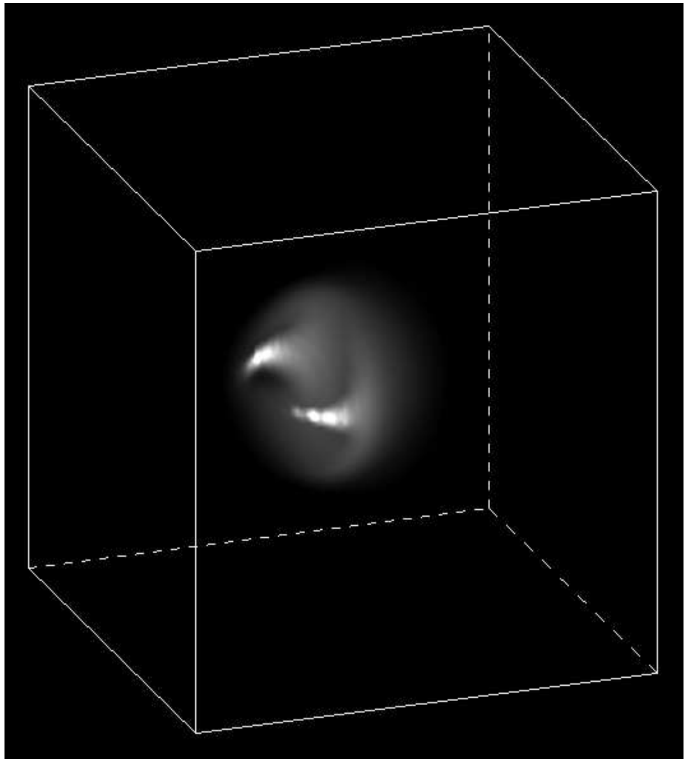

Simulation of 3D amplitude equations from an initial Alfvén wave packet of amplitude $B_0 = 6e^{-[\frac{1}{25}(x-5\pi)^2+2.5(y-\pi)^2+(z-\pi)^2]}$.

Simulation of 3D Hall-MHD (1024x128x256)

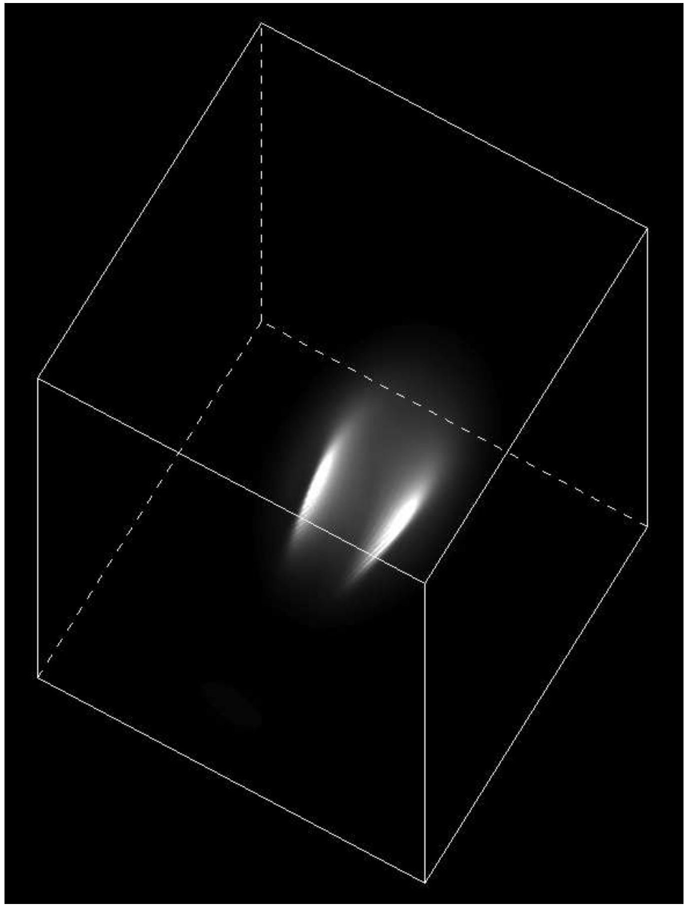

Direct simulation of an Alfvén wave packet with an initial amplitude $e^{-\frac{1}{288}[\frac{1}{25}(x-48\pi)^2+(y-10\pi)^2+2.25(z-10\pi)^2]}$.

VI. Retaining kinetic effects in a fluid description of long Alfvén waves

In natural and fusion plasmas, collisions usually negligible.

Description of the large-scale dynamics in terms of usual magnetohydrodynamics questionable.

In most situations, direct numerical integration of the Vlasov-Maxwell equations beyond the capabilities of the present day computers.

This suggest development of a reduced description of the large-scale dynamics that retains most of the aspects of a fluid description but includes realistic approximations of the pressure tensor and wave-particle resonances.

Rogister (Phys. Fluids **14**, *2733 (1971))*: reductive perturbative expansion on the Vlasov-Maxwell equations to isolate the dynamics of small-amplitude Alfvén waves with a typical length much larger than the ion inertial length.

Here we revisit Rogister's approach and generalize it to address transverse phenomena, such as the filamentation of a small-amplitude Alfvén wave train.

V.a Derivation of the KDNLS equation

Vlasov-Maxwell equations:

$$\partial_t f_r + v \cdot \nabla f_r + \frac{q_r}{m_r}(e + \frac{1}{c} v \times b) \cdot \nabla_v f_r = 0$$

$$\frac{1}{c}\partial_t b = -\nabla \times e$$

$$\nabla \times b = \frac{4\pi}{c} \sum_r q_r n_r \int v f_r d^3 v + \frac{1}{c}\partial_t e$$

$$\nabla \cdot e = 4\pi \sum_r q_r n_r \int f_r d^3 v,$$

f_r and n_r are the distribution function and the average number density of the particle species r with charge q_r and mass m_r. The electric and magnetic fields are e and b respectively.

For an ambient field of strength B_0 pointing in the x-direction,

$$\xi = \epsilon^2 (x - \lambda t)$$

$$\eta = \epsilon^3 y \quad , \quad \zeta = \epsilon^3 z$$

$$\tau = \epsilon^4 t$$

λ is the Alfvén-wave propagation velocity (to be determined)

$$f_r = F_r^{(0)} + \epsilon(f_r^{(0)} + \epsilon f_r^{(1)} + \ldots)$$
$$b = B_0 \widehat{x} + \epsilon(b^{(0)} + \epsilon b^{(1)} + \ldots)$$
$$e = \epsilon(e^{(0)} + \epsilon e^{(1)} + \ldots),$$

Equilibrium velocity distribution function $F_r^{(0)}$ is rotationally symmetric around the direction of the ambient field and symmetric relatively to the parallel velocity component.

$\widehat{x}$: unit vector in the direction of the ambient magnetic field.

Cyclotron frequency of the particles of species r: $\Omega_r = \frac{q_r B_0}{m_r c}$

Velocity: $v = (v_{||} \; , \; v_\perp \cos\phi \; , \; v_\perp \sin\phi)$

Expand Vlasov equation:

$$\Omega_r \partial_\phi F_r^{(0)} = 0$$

$$\Omega_r \partial_\phi f_r^{(0)} = \Sigma_r^{(0)}$$

$$\Omega_r \partial_\phi f_r^{(1)} = \Sigma_r^{(1)}$$

$$\Omega_r \partial_\phi f_r^{(2)} = (v_\| - \lambda)\partial_\xi f_r^{(0)} + \Sigma_r^{(2)}$$

$$\Omega_r \partial_\phi f_r^{(3)} = (v_\| - \lambda)\partial_\xi f_r^{(1)} + (\vec{v}_\perp \cdot \nabla_\perp) f_r^{(0)} + \Sigma_r^{(3)}$$

$$\Omega_r \partial_\phi f_r^{(4)} = (v_\| - \lambda)\partial_\xi f_r^{(2)} + (\vec{v}_\perp \cdot \nabla_\perp) f_r^{(1)} + \partial_\tau f_r^{(0)} + \Sigma_r^{(4)}$$

$$\Omega_r \partial_\phi f_r^{(5)} = (v_\| - \lambda)\partial_\xi f_r^{(3)} + (\vec{v}_\perp \cdot \nabla_\perp) f_r^{(2)} + \partial_\tau f_r^{(1)} + \Sigma_r^{(5)}$$

where

$$\Sigma_r^{(s)} = \frac{q_r}{m_r}(e^{(s)} + \frac{1}{c} v \times b^{(s)}) \cdot \nabla_v F_r^{(0)} + \sum_{p+q=s-1} \frac{q_r}{m_r}(e^{(p)} + \frac{1}{c} v \times b^{(p)}) \cdot \nabla_v f_r^{(q)},$$

the second term of the r.h.s. being absent when $s = 0$.

Solvability condition for $f_r^{(3)}$:

$(v_\parallel - \lambda)\partial_\xi \overline{f}_r^{(1)} = (v_\parallel - \lambda) R_r + S_r \frac{\partial F_r^{(0)}}{\partial v_\parallel}$ with $\overline{f}_r^{(1)} = \frac{1}{2\pi}\int f_r^{(1)} d\phi$ where S_r is independent of $v_\parallel$.

Wave-particle resonance at $v_\parallel = \lambda$: LANDAU KINETIC EFFECT

$$\int \partial_\xi \overline{f}_r^{(1)} dv_\parallel = \int R_r dv_\parallel + P\int \frac{1}{v_\parallel - \lambda}\frac{\partial F_r^{(0)}}{\partial v_\parallel} dv_\parallel S_r + \pi \frac{\partial F_r^{(0)}}{\partial v_\parallel}|_{v_\parallel = \lambda} \mathcal{H}_\xi\{S_r\}$$

where $\mathcal{H}_\xi$ is the Hilbert transform with respect to the longitudinal coordinate.

From Maxwell equations:

Local magnetic field:

$$b = \left(B_0 + \epsilon^2 b_\parallel^{(1)} + \cdots \ , \ \epsilon(b_\perp^{(0)} + \epsilon^2 b_\perp^{(2)} + \cdots)\right) + O(\epsilon^3)$$

$$\partial_\xi b_\parallel^{(1)} + \nabla_\perp b_\perp^{(0)} = 0$$

$$|b| = B_0(1 + \epsilon^2 A) + O(\epsilon^3) \quad , \quad A = \frac{b_\parallel^{(1)}}{B_0} + \frac{|b_\perp^{(0)}|^2}{2B_0^2}$$

Electric field:

$$e_\perp = -\epsilon\frac{\lambda}{c}\widehat{x}\times b_\perp^{(0)} + \epsilon^3(-\frac{\lambda}{c}\widehat{x}\times b_\perp^{(2)} + \frac{1}{c}\widehat{x}\times\partial_\xi^{-1}\partial_\tau b_\perp^{(0)}) + \cdots$$

$$e_\parallel = \epsilon^4(\frac{1}{cB_0}b_\perp^{(0)}\times\partial_\xi^{-1}\partial_\tau b_\perp^{(0)} + \mathcal{L}^{-1}\mathcal{M}\,\partial_\xi A) + \cdots$$

where

$$\mathcal{L} = 2\pi\sum_r \frac{q_r^2 n_r}{m_r}\int_0^\infty d(\frac{v_\perp^2}{2})\,\mathcal{G}_r \quad , \quad \mathcal{M} = 2\pi\sum_r q_r n_r\int_0^\infty d(\frac{v_\perp^2}{2})\frac{v_\perp^2}{2}\,\mathcal{G}_r$$

$$\mathcal{G}_r = \mathrm{P}\int \frac{1}{v_\parallel-\lambda}\frac{\partial F_r^{(0)}}{\partial v_\parallel}\,dv_\parallel + \pi\frac{\partial F_r^{(0)}}{\partial v_\parallel}\,|_{v_\parallel=\lambda}\mathcal{H}_\xi$$

$$\mathcal{H}_\xi\{S\} = \frac{1}{\pi}\mathrm{P}\int\frac{S(\xi')}{\xi'-\xi}d\xi'$$

One gets the dynamical equation

$$\partial_\tau b_\perp^{(0)} + \delta \partial_{\xi\xi}(\widehat{x} \times b_\perp^{(0)}) - \frac{B_0}{2\lambda\rho^{(0)}}\nabla_\perp \widetilde{P} + \frac{\partial}{\partial \xi}[(\frac{\widetilde{P}}{2\lambda\rho^{(0)}} + \langle U \rangle_\xi) b_\perp^{(0)}] = 0$$

dispersion coefficient: $\delta = \frac{1}{2\Omega_i}(\lambda^2 + 3\frac{p_{\parallel i}^{(0)}}{\rho^{(0)}} - 2\frac{p_{\perp i}^{(0)}}{\rho^{(0)}})$

Propagation velocity: $\lambda = [\frac{1}{\rho^{(0)}}(\frac{1}{4\pi}|B_0|^2 + p_\perp^{(0)} - p_\parallel^{(0)})]^{\frac{1}{2}}.$

$$\widetilde{P} = \frac{B_0^2}{4\pi}\widetilde{A} + (2p_\perp^{(0)} + \mathcal{N} - \mathcal{M}^2\mathcal{L}^{-1})\widetilde{A} = \widetilde{p}_{mag}^{(1)} + \widetilde{p}_\perp^{(1)}$$

$$\mathcal{N} = 2\pi \sum_r m_r n_r \int_0^\infty d(\frac{v_\perp^2}{2})\frac{v_\perp^4}{4}\mathcal{G}_r.$$

$\psi = \langle \psi \rangle_\xi + \widetilde{\psi}$, $\langle \cdot \rangle_\xi$: averaging on the ξ-variable.

$\langle b_\perp^{(0)} \rangle_\xi = 0$ (not driven by the dynamics).

The mean values arise when solving equations of the form $\partial_\xi \psi = 0$.

In the case of LOCALIZED ALFVÉN WAVE PULSE, all the functions decay to zero as $\xi \to \pm\infty$. The mean values $\langle \cdot \rangle_\xi$ are also zero and THE SYSTEM IS CLOSED (*Rogister 1971*).

Such a "Kinetic Derivative Non-Linear Schrödinger" equation can be reproduced by a long-wave reductive perturbative expansion performed on the Hall-MHD equations with pressure fluctuations computed using the guiding center approximation *(Mjølhus and Wyller, J. Plasma Phys.* **40**, *299 (1988))*.

Mean field contributions are to be computed when dealing with Alfvén wave trains. Their role is essential for describing the phenomenon of Alfvén wave filamentation.

$$\langle U\rangle_\xi = \langle u_\parallel^{(1)}\rangle_\xi + \frac{\lambda}{2B_0}\langle b_\parallel^{(1)}\rangle_\xi + \frac{1}{\lambda\rho^{(0)}}(p_\parallel^{(0)} - p_\perp^{(0)})\langle A\rangle_\xi + \frac{1}{2\lambda\rho^{(0)}}(\langle p_\perp^{(1)}\rangle_\xi - \langle p_\parallel^{(1)}\rangle_\xi)$$

$$\partial_\tau\langle u_\parallel^{(1)}\rangle_\xi = \frac{1}{\rho^{(0)}B_0}\nabla_\perp\cdot\langle\widetilde{P}b_\perp^{(0)}\rangle_\xi \qquad \widetilde{P} = \frac{B_0^2}{4\pi}\widetilde{A} + \widetilde{p}_\perp^{(1)}$$

$$\langle p_\perp^{(1)}\rangle_\xi + \frac{B_0^2}{4\pi}\langle A\rangle_\xi = \Pi(\tau) \qquad A = \frac{b_\parallel^{(1)}}{B_0} + \frac{|b_\perp^{(0)}|^2}{2B_0^2}$$

where

$$\frac{d}{d\tau}\Pi(\tau) = -\frac{1}{2\lambda\rho^{(0)}}(\frac{B_0^2}{4\pi} + p_\perp^{(0)})\langle\widetilde{A}(\mathcal{N} - \mathcal{M}^2\mathcal{L}^{-1})\partial_\xi\widetilde{A}\rangle_{\xi,\eta,\zeta}$$

This constraint defines $\langle b_\parallel^{(1)}\rangle_\xi$ in terms of the transverse magnetic field and of the mean transverse pressure.

Transverse and parallel $O(\epsilon^2)$-pressure perturbations (relatively to the local magnetic field):

Fluctuating parts:

$$\widetilde{p}_{\perp}^{(1)} = (2p_{\perp}^{(0)} + \mathcal{N} - \mathcal{M}^2\mathcal{L}^{-1})\widetilde{A}$$

$$\widetilde{p}_{\parallel}^{(1)} = (p_{\parallel}^{(0)} - p_{\perp}^{(0)})\widetilde{A} + \lambda^2(\widetilde{\rho}^{(1)} - \rho^{(0)}\widetilde{A})$$

$$\widetilde{\rho}^{(1)} = (\rho^{(0)} + \mathcal{O} - \mathcal{P}\mathcal{L}^{-1}\mathcal{M})\widetilde{A}$$

$$\mathcal{O} = 2\pi\sum_r m_r n_r \int_0^\infty \frac{v_\perp^2}{2}\mathcal{G}_r d(\frac{v_\perp^2}{2}) \quad , \quad \mathcal{P} = 2\pi\sum_r q_r n_r \int_0^\infty \mathcal{G}_r d(\frac{v_\perp^2}{2}),$$

Equations for the mean pressures:

$$\partial_\tau\left(\frac{\langle p_{\perp}^{(1)}\rangle_\xi}{p_{\perp}^{(0)}} - \frac{\langle\rho^{(1)}\rangle_\xi}{\rho^{(0)}} - \langle A\rangle_\xi\right) = 0$$

$$\partial_\tau\left(\frac{\langle p_{\parallel}^{(1)}\rangle_\xi}{p_{\parallel}^{(0)}} - 3\frac{\langle\rho^{(1)}\rangle_\xi}{\rho^{(0)}} + 2\langle A\rangle_\xi\right) = \frac{2\lambda}{p_{\parallel}^{(0)}}\langle\widetilde{A}(\mathcal{N} - \mathcal{M}^2\mathcal{L}^{-1})\partial_\xi\widetilde{A}\rangle_\xi$$

with

$$\langle\frac{\rho^{(1)}}{\rho^{(0)}}\rangle_\xi = \langle\frac{b_{\parallel}^{(1)}}{B_0}\rangle_\xi$$

This leads to a CLOSED SYSTEM:

$$\left(\partial_\tau + \langle U\rangle_\xi \partial_\xi\right) b_\perp^{(0)} + \frac{\partial}{\partial\xi}(\frac{\widetilde{P} b_\perp^{(0)}}{2\lambda\rho^{(0)}}) - \frac{B_0}{2\lambda\rho^{(0)}}\nabla_\perp \widetilde{P} + \delta\partial_{\xi\xi}\left(\widehat{x} \times b_\perp^{(0)}\right) = 0$$

$$\rho^{(0)}\partial_\tau \langle U\rangle_\xi = c_1 \left(\nabla_\perp \cdot \langle \widetilde{P}\frac{b_\perp^{(0)}}{B_0}\rangle_\xi - \langle \widetilde{A}\mathcal{K}\partial_\xi \widetilde{A}\rangle_\xi \right) - c_2 \langle \widetilde{A}\mathcal{K}\partial_\xi \widetilde{A}\rangle_{\xi,\eta,\zeta},$$

$$\partial_\xi \widetilde{b}_\parallel^{(1)} + \nabla_\perp \cdot b_\perp^{(0)} = 0$$

$$\widetilde{P} = (\frac{B_0^2}{4\pi} + 2p_\perp^{(0)} + \mathcal{K})\widetilde{A}$$

with $A = \frac{b_\parallel^{(1)}}{B_0} + \frac{|b_\perp^{(0)}|^2}{2B_0^2} \quad , \quad \mathcal{K} = \mathcal{N} - \mathcal{M}^2\mathcal{L}^{-1},$

$$c_1 = \frac{1}{2+\beta_\perp - \beta_\parallel}(\frac{12 + 18\beta_\perp + 5\beta_\perp^2}{8(1+\beta_\perp)}) \quad , \quad c_2 = \frac{1}{2+\beta_\perp - \beta_\parallel}(\frac{(2+\beta_\perp)^2}{8(1+\beta_\perp)})$$

where $\beta_\parallel = 8\pi p_\parallel^{(0)}/B_0^2$ and a similar definition in the perpendicular direction.

V.b Landau damping of circularly polarized Alfvén wave trains

In one dimension the KDNLS equation writes

$$\partial_\tau b + \frac{\partial}{\partial \xi}(b(\alpha + \gamma \mathcal{H})|b|^2) + i\delta \frac{\partial^2}{\partial \xi^2} b = 0$$

When $|b|^2$ is constant, there is no Landau damping: the $\mathcal{H}$ term vanishes. However it is non zero in presence of modulation, hence the misleading denomination of nonlinear Landau damping.

Two main points (Fla, Mjølhus and Wyller, Physica Scripta **40**, 219 (1989)):

- Instability of the circularly polarized wave for all parameter values (even RH polarization, $\beta < 1$, although it is weak in that case).
- For typical parameters instability of the RH case is suppressed for $\beta > 1$.

Also: along with damping, wavenumber decreases, a consequence of the conservation of helicity $K = \frac{1}{2i}\int_{-\infty}^{+\infty} [b^\star \int_{-\infty}^{x} b dx' - b \int_{-\infty}^{x} b^\star dx'] dx = -2\pi \mathcal{P} \int_{-\infty}^{+\infty} \frac{|b_k|^2}{k} dk.$

Numerical simulations show the formation of stationary S-type and arc-polarized directional and rotational discontinuities (Medvedev et al. PRL **78**, 4934 (1997)). Linear waves evolve to rotational discontinuities while circular ones do not evolve, a phenomenon due to the fact that Landau damping is NOT restricted to small scales.

V.c Filamentation in collisionless plasmas

Derive an envelope equation from KDNLS with mean fields:

Define slow transverse variables $Y = \varepsilon\eta$ and $Z = \varepsilon\zeta$ and slow time $T = \varepsilon^2\tau$;

Consider a circularly polarized quasi-monochromatic Alfvén wave train, slowly modulated in the transverse directions:

$b_\perp^{(0)} = \varepsilon\psi(Y, Z, T)e^{i(k\xi-\omega\tau)}$.

Up to a simple rescaling, the wave envelope obeys a nonlinear Schrödinger equation with dissipation

$$i\partial_T\psi + (\chi + i\nu)\Delta_\perp\psi - k(\frac{\lambda}{B_0^2}(c_1|\psi|^2 + c_2\langle\langle|\psi|^2\rangle\rangle - c_1|\psi_0|^2 - c_2\langle\langle|\psi_0|^2\rangle\rangle))\psi = 0$$

with $\chi = \frac{v_A^2}{4k\lambda}(1 + \beta_\perp + \frac{K_R}{\rho^{(0)}v_A^2})$ and $\nu = \frac{K_I}{4|k|\lambda\rho^{(0)}}$

where $\mathcal{K} = K_R + K_I\mathcal{H}$ and $v_A = \frac{B_0^2}{4\pi\rho^{(0)}}$.

Dispersion relation for a monochromatic perturbation $e^{i(KX-\Omega T)}$ of a wave of amplitude $|\psi_0|$:

$$\Omega = i\nu K^2 \pm \sqrt{2\chi k\lambda c_1 \frac{|\psi_0|^2}{B_0^2} K^2 + \chi^2 K^4}.$$

Instability for negative μ.

• When $T_\perp = T_\parallel$ for both ions and electrons with $T_p = T_e$,
No filamentation instability

• When $T_\perp = T_\parallel$ for both ions and electrons with $T_p \ll T_e$,
$\chi^* = \chi(\frac{v_A^2}{4k\lambda})^{-1}$ reduces to $\chi^* = \dfrac{1}{1-\beta}$ with $\beta = \frac{T_e}{m_p\lambda^2}$.

In this limit, filamentation occurs for $\beta > 1$.

Effect of the ratio electron vs. ion temperature

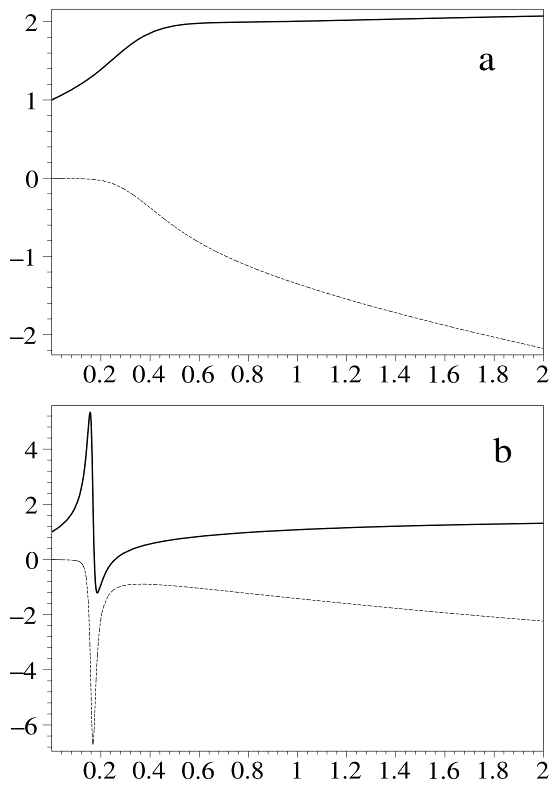

Figure 20: Plots of χ^* (solid line) and ν^* (dashed line) as a function of $\beta_{\|p}$ when all temperatures are equal (a) and when $T_e = 8T_p$ (b).

Effect of electron temperature anisotropy

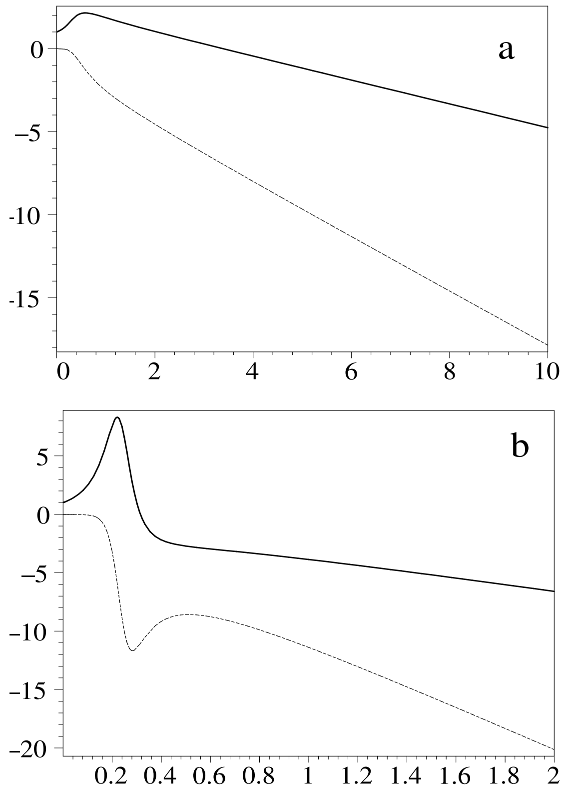

Figure 21: Plots of χ^* (solid line) and ν^* (dashed line) as a function of $\beta_{\|p}$ for $T_{\perp e} = 1.8T_{\|e}$ (a) and for 10% of He^{2+} with $T_{\perp p} = 3.25T_{\|p}$, $T_{\perp\alpha} = 3.25T_{\|\alpha}$, $T_{\perp e} = 1.27T_{\|e}$, $T_{\|e} = 5.5T_{\|p}$, $T_{\|\alpha} = 5.5T_{\|\alpha}$ (b). These parameters are typical of the solar wind; filamentation takes place as soon as $\beta_{\|p}$ exceeds a critical value $\beta_c = 0.315$.

Variation of β_c as functions of electron temperature anisotropy and ratio of electron to proton temperature

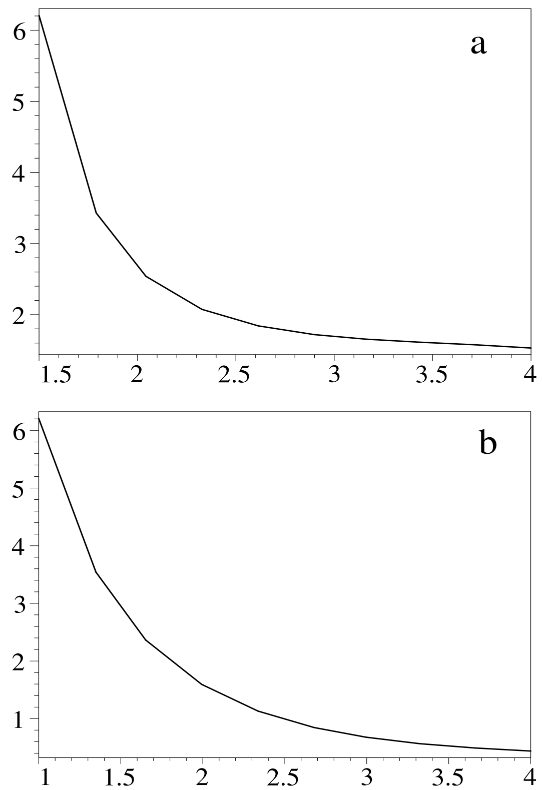

Figure 22: Plot of the critical value β_c as a function of $T_{\perp e}/T_{\| e}$ for $T_{\perp p} = T_{\| p}$, $T_{\| e} = T_{\| p}$ (a) and as a function of $T_{\| e}/T_{\| p}$ for $T_{\perp p} = T_{\| p}$, $T_{\perp e} = 1.5 T_{\| e}$ (b).

VII. A Landau-fluid model for dispersive MHD waves

From Vlasov-Maxwell equations, derive a hierarchy of moment equations for each particle species r:

density $\rho_r = m_r n_r \int f_r d^3v$
hydrodynamic velocity $u_r = n_r \int v f_r d^3v$
pressure tensor $P_r = m_r n_r \int (v - u_r) \otimes (v - u_r) f_r d^3v$
heat flux tensor $Q_r = m_r n_r \int (v - u_r) \otimes (v - u_r) \otimes (v - u_r) f_r d^3v$.

$$\partial_t \rho_r + \nabla \cdot (u_r \rho_r) = 0$$

$$\partial_t u_r + u_r \cdot \nabla u_r + \frac{1}{\rho_r} \nabla \cdot P_r - \frac{q_r}{m_r}(e + \frac{1}{c} u_r \times b) = 0$$

$$\partial_t P_r + \nabla \cdot (u_r P_r + Q_r) = 2[P_r \cdot \nabla u_r + \frac{q_r}{m_r c} b \times P_r]^{\mathcal{S}}$$

$[\cdot]^{\mathcal{S}}$ is the symmetric part of the corresponding matrix.

Large-scale dynamics: $\Omega_r = \frac{q_r B_0}{m_r c} \to \infty$:

Pressure tensor $P_r = P_r^0 + P_r^{(1)} + \cdots$

Gyrotropic pressure: $P_r^{(0)} = p_{\perp r}(I - \widehat{b} \otimes \widehat{b}) + p_{\| r} \widehat{b} \otimes \widehat{b}$

Gyrotropic heat flux:
$Q^{(0)}_{ijk,r} = q_{\| r} \widehat{b}_i \widehat{b}_j \widehat{b}_k + q_{\perp r}(\delta_{ij} \widehat{b}_k + \delta_{ik} \widehat{b}_j + \delta_{jk} \widehat{b}_i - 3 \widehat{b}_i \widehat{b}_j \widehat{b}_k)$,

$$\partial_t p_\perp + \nabla \cdot (u_r\, p_{\perp r}) + \nabla \cdot (\widehat{b}\, q_{\perp r}) + p_{\perp r} \nabla \cdot u_r - p_{\perp r}\, \widehat{b} \cdot \nabla u_r \cdot \widehat{b} + q_{\perp r} \nabla \cdot \widehat{b} = 0$$
$$\partial_t p_{\| r} + \nabla \cdot (u_r\, p_{\| r}) + \nabla \cdot (\widehat{b}\, q_{\| r}) + 2 p_{\| r}\, \widehat{b} \cdot \nabla u_r \cdot \widehat{b} - 2 q_{\perp r} \nabla \cdot \widehat{b} = 0$$

Heat fluxes in the long-wave asymptotics

When the plasma contains electrons and only one species of $Z = 1$ ions with bi-maxwellian equilibrium distribution functions, operators $\mathcal{L}$, $\mathcal{M}$, $\mathcal{N}$ are expressed in terms of the plasma response function

$$\mathcal{W}_r \equiv \mathcal{W}(c_r) = \frac{1}{\sqrt{2\pi}} \mathrm{P} \int \frac{\zeta e^{-\zeta^2/2}}{\zeta - c_r} d\zeta + \sqrt{\frac{\pi}{2}} c_r e^{-c_r^2/2} \mathcal{H}_\xi,$$

where $c_r = \lambda / v_{th,r}$ and $v_{th,r} = \sqrt{T^{(0)}_{\| r} / m_r}$.

One has

$$\frac{q^{(1)}_{\| r}}{v_{th,r} p^{(0)}_{\| r}} = \frac{c_r (c_r^2 - 3 + \mathcal{W}_r^{-1})}{c_r^2 - 1 + \mathcal{W}_r^{-1}} \frac{T^{(1)}_{\| r}}{T^{(0)}_{\| r}}$$
$$\frac{q^{(1)}_{\perp r}}{v_{th,r} p^{(0)}_{\perp r}} = -\frac{T^{(0)}_{\perp r}}{T^{(0)}_{\| r}} \frac{c_r \mathcal{W}_r}{1 - \frac{T^{(0)}_{\perp r}}{T^{(0)}_{\| r}} \mathcal{W}_r} \frac{T^{(1)}_{\perp r}}{T^{(0)}_{\perp r}} = -\frac{T^{(0)}_{\perp r}}{T^{(0)}_{\| r}} c_r \mathcal{W}_r A$$

In the nearly isothermal limit ($c_r \ll 1$), $\mathcal{W}_r \approx 1 - c_r^2 + \sqrt{\frac{\pi}{2}} c_r \mathcal{H}_\xi$.
$q_{\parallel r}^{(1)} = -\sqrt{\frac{8}{\pi}} v_{th,r} n^{(0)} \mathcal{H}_\xi T_{\parallel r}^{(1)}$ and $q_{\perp r}^{(1)} \ll 1$.

In the adiabatic limit ($c_r \gg 1$), $\mathcal{W}_r \approx -1/c_r^2 - 3/c_r^4$.
Heat fluxes are negligible.

Towards a Landau fluid closure

Extension to more general situations:

- c_r replaced by $-\frac{1}{v_{th,r}}\partial_t\partial_x^{-1}$.

- equations for the heat fluxes replaced by

$$\frac{q^{(1)}_{\parallel r}}{v_{th,r}p^{(0)}_{\parallel r}} = \mathcal{F}_\parallel(-\frac{1}{v_{th,r}}\partial_t\partial_x^{-1})\frac{T^{(1)}_{\parallel r}}{T^{(0)}_{\parallel r}}$$

$$\frac{q^{(1)}_{\perp r}}{v_{th,r}p^{(0)}_{\perp r}} = \mathcal{F}^1_\perp(-\frac{1}{v_{th,r}}\partial_t\partial_x^{-1})\frac{T^{(1)}_{\perp r}}{T^{(0)}_{\perp r}} + \mathcal{F}^2_\perp(-\frac{1}{v_{th,r}}\partial_t\partial_x^{-1})A$$

with homographic approximants

$$\mathcal{F}_\parallel(X) = (q^3_\parallel + q^4_\parallel X\mathcal{H})^{-1}(q^1_\parallel X + q^2_\parallel \mathcal{H})$$

$$\mathcal{F}^1_\perp(X) = (q^3_\perp + q^4_\perp X\mathcal{H})^{-1}(q^1_\perp X + q^2_\perp \mathcal{H})$$

$$\mathcal{F}^2_\perp(X) = (q^3_\perp + q^4_\perp X\mathcal{H})^{-1}(q^5_\perp X + q^6_\perp \mathcal{H}).$$

The coefficients $q^i_\parallel$ and $q^i_\perp$ are chosen in a way that ensures the correct asymptotic behavior of the heat fluxes in both isothermal ($c_r \ll 1$) and adiabatic ($c_r \gg 1$) limits.

The Landau-fluid model

For a plasma of electrons and one ion species with $Z = 1$, velocity $u = u_i = u_e$ and density $\rho = \sum_r \rho_r = n \sum_r m_r$ obey

$$\partial_t \rho + \nabla \cdot (u\rho) = 0$$

$$\rho\,(\partial_t u + u \cdot \nabla u) + \nabla \cdot (P^{(0)} + \Pi) - \frac{1}{4\pi}(\nabla \times b) \times b = 0.$$

with $P^{(0)} = \sum_r P_r^{(0)}$ and finite Lamor radius corrections

$$\Pi_{yy} = -\Pi_{zz} = -\frac{p_{\perp i}}{2\Omega_i}(\partial_y u_z + \partial_z u_y)$$

$$\Pi_{xx} = 0$$

$$\Pi_{yz} = \Pi_{zy} = \frac{p_{\perp i}}{2\Omega_i}(\partial_y u_y - \partial_z u_z)$$

$$\Pi_{zx} = \Pi_{xz} = -\frac{1}{\Omega_i}[p_{\perp i}(\partial_x u_y - \partial_y u_x) - 2p_{\| i}\partial_x u_y]$$

$$\Pi_{xy} = \Pi_{yx} = \frac{1}{\Omega_i}[p_{\perp i}(\partial_x u_z - \partial_z u_x) - 2p_{\| i}\partial_x u_z].$$

Parallel and perpendicular gyrotropic pressures governed by

$$\partial_t p_{\| r} + \nabla \cdot (u\, p_{\| r} + \widehat{b}\, q_{\| r}) + 2p_{\| r}\,\widehat{b} \cdot \nabla u \;\cdot \widehat{b} - 2q_{\perp r} \nabla \cdot \widehat{b} = 0,$$

$$\partial_t p_{\perp r} + \nabla \cdot (u\, p_{\perp r} + \widehat{b}\, q_{\perp r}) + p_{\perp r} \nabla \cdot u - p_{\perp r}\,\widehat{b} \cdot \nabla u \cdot \widehat{b} + q_{\perp r} \nabla \cdot \widehat{b} = 0.$$

Induction equation with Hall-effect and electron pressure

$$\partial_t b - \nabla \times (u \times b) = -\frac{m_i c}{q_i} \nabla \times [\frac{1}{4\pi\rho}(\nabla \times b) \times b - \frac{1}{\rho} \nabla \cdot P_e^{(0)}].$$

Heat flux closures

$$(\frac{d}{dt} + \frac{v_{th,r}}{\sqrt{\frac{8}{\pi}}(1 - \frac{3\pi}{8})} \mathcal{H} \nabla_{\|}) \frac{q_{\| r}}{v_{th,r} p_{\|}^{(0)}} = \frac{1}{1 - \frac{3\pi}{8}} v_{th,r} \nabla_{\|} \frac{T_{\| r}}{T_{\| r}^{(0)}}$$

$$(\frac{d}{dt} - \sqrt{\frac{\pi}{2}} v_{th,r} \mathcal{H} \nabla_{\|}) \frac{q_{\perp r}}{v_{th,r} p_{\perp r}^{(0)}} = -v_{th,r} \nabla_{\|} (\frac{T_{\perp r}}{T_{\perp r}^{(0)}} + (\frac{T_{\perp r}^{(0)}}{T_{\| r}^{(0)}} - 1) \frac{|b|}{B_0}),$$

with $p_{\| r} = n T_{\| r}$ and $p_{\perp r} = n T_{\perp r}$.

Landau-fluid description of long dispersive Alfvén waves

The long wave reductive perturbative expansion performed on the Landau-fluid model reproduces the KDNLS equations derived from Vlasov-Maxwell up to the replacement in the transverse pressure fluctuations of $\mathcal{K} = \mathcal{N} - \mathcal{M}^2\mathcal{L}^{-1}$ by $\frac{\mathcal{N}_2+\mathcal{N}_4}{2} - \mathcal{M}_4^2\mathcal{L}_4^{-1}$ where the subscripts in the operators correspond to the replacement of the plasma response function $\mathcal{W}$ by the corresponding two- or four-pole approximants.

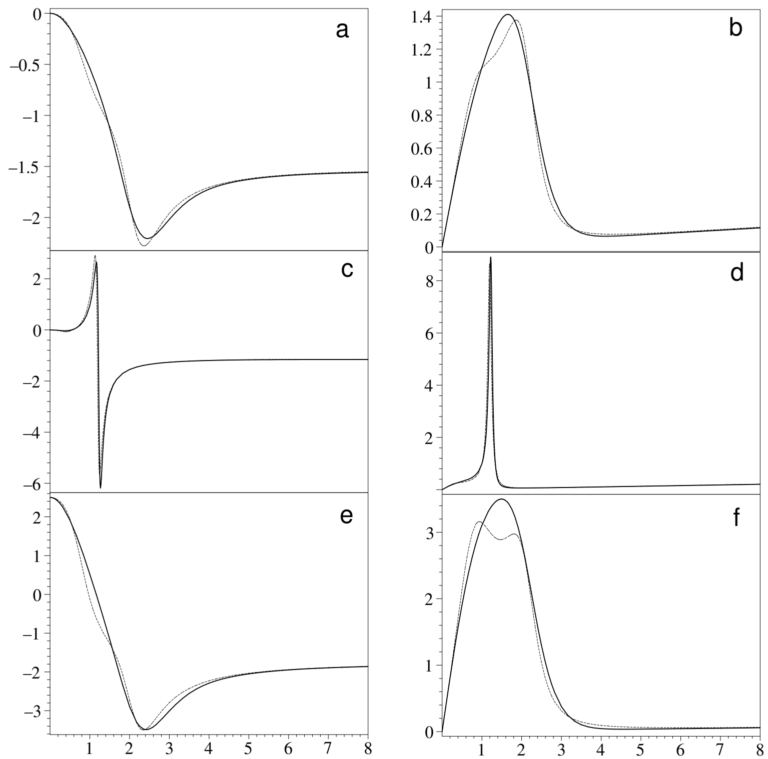

Figure 23: Contributions p^R (left column) and p^I (right column) to the perpendicular pressure $\frac{\widetilde{p}_\perp^{(1)}}{p_\perp^{(0)}} = -(p^R + p^I \mathcal{H})\widetilde{A}$ versus $\beta^{-1/2}$, where $\beta = T_{\|e}/(m_i \lambda^2)$, for $T_{\|e} = T_{\|i} = T_{\perp e} = T_{\perp i}$ (a and b), for $T_{\|e} = 8T_{\|i}$ and $T_{\perp e} = T_{\|e}$, $T_{\perp i} = T_{\|i}$ (c,d) and for $T_{\perp e} = T_{\|e} = T_{\|i}$ and $T_{\perp i} = 3T_{\|i}$ (e, f). The solid line refers to the exact (long wave) kinetic calculation and the dashed line to the Landau-fluid closure.

An extended Hall Landau-fluid model has also been built that reproduces the dynamics of long obliquely propagating waves.

- For magnetosonic waves, the Landau damping rate (assuming $\frac{m_e}{m_p} \ll \beta \ll \frac{T_e}{T_p}$) is

$$\gamma = -\sqrt{\beta}\sqrt{\frac{\pi}{8}}\sqrt{\frac{m_e}{m_p}}\frac{\sin^2\alpha}{\cos\alpha}\frac{(\omega^2-\beta\cos^2\alpha)^2+\beta^2\cos^4\alpha}{(2\omega^2-\beta-1)(\omega^2-\beta\cos^2\alpha)},$$

an expression identical to that found in Akhiezer (Vol. 1). The long-wave equation is KdV+damping term.

- For Alfvén waves at finite angle of propagation , finite Larmor radius corrections of order $1/\Omega_p^2$ have to be added. The governing equation is linear and reads, assuming $\frac{m_e}{m_p} \ll \beta \ll \frac{T_e}{T_p}$, (adiabatic protons and isothermal electrons) and $\beta \ll 1$

$$\partial_\tau \frac{b_y}{B_0} + \frac{v_A^3}{2\Omega_p^2}[\frac{\cos^3\alpha}{\sin^2\alpha} + \sqrt{\beta}\sqrt{\frac{\pi}{2}}\sqrt{\frac{m_e}{m_p}}\cos^3\alpha(\tan^2\alpha + \frac{1}{\tan^2\alpha})\mathcal{H}]\partial_{\xi\xi\xi}\frac{b_y}{B_0} = 0,$$

- For Kinetic Alfvén waves $(\cos^2\theta \ll \beta)$,

$$\partial_\tau \frac{b_y}{B_0} + \frac{v_A^3}{2\Omega_p^2}\cos\theta[-\beta(1+\frac{3}{4}\frac{T_p^{(0)}}{T_e^{(0)}}) + \sqrt{\beta}\sqrt{\frac{\pi}{2}}\sqrt{\frac{m_e}{m_p}}\mathcal{H}]\partial_{\xi\xi\xi}\frac{b_y}{B_0} = 0.$$

VIII. Conclusion

Collisionless dissipation (Landau damping) of dispersive MHD waves can be described using a fluid model.

The model thus reproduces the correct dispersion relation for MHD waves for any value of the β parameter and for any angle of propagation, provided the wavelength is large compared to the ion inertial length.

Secondary instabilities as well as the resulting nonlinear dynamics are also captured.

For example small-amplitude oblique Alfvén waves obey a linear dynamics while parallel Alfvén waves are governed by the KDNLS equation.

In particular, Alfvén wave filamentation occurs for $\beta_{\|p} > \beta_c$ where β_c is of order unity as soon as $T_{\perp e} \geq T_{\|e}$ and/or $T_{\|e} > T_{\|p}$. The value β_c can become small when $T_{\perp e} > T_{\|e}$ increases.

Perspectives

• Simulation of dispersive Alfvén wave turbulence:

⋆ Generation of KAW at small scales: importance of higher-order FLR corrections that are to be described in a computationally manageable way.

⋆ Self-consistent computation of turbulent dissipation

⋆ Possible emergence of coherent structures

• Treat electrons as a Landau fluid in hybrid simulations.

• Explore the possible description of nonlinear Landau damping (see Prakash and Diamond, Nonlinear Proc. Geophys. **6**, 161 (1999)).

References:

Passot T. and Sulem, P.L.: A long-wave model for Alfvén wave trains in a collisionless plasma: I. Kinetic theory, Phys. Plasmas, in press.

Passot T. and Sulem, P.L.: A long-wave model for Alfvén wave trains in a collisionless plasma: II. A Landau-fluid approach, Phys. Plasmas, in press.

T. Passot and P.L. Sulem, "Filamentation instability of long Alfvén waves in warm collisionless plasmas", Phys. Plasmas, in press.

T. Passot and P.L. Sulem, "A fluid description for Landau damping of dispersive MHD waves", submitted to Nonlinear Proc. Geophys.